Complete Assignment of Cytochrome *c* Resonance Raman Spectra via Enzymatic Reconstitution with Isotopically Labeled Hemes

Songzhou Hu,[†] Ian K. Morris,[‡] Jai P. Singh,[‡] Kevin M. Smith,[‡] and Thomas G. Spiro*,[†]

Contribution from the Departments of Chemistry, Princeton University, Princeton, New Jersey 08544, and University of California, Davis, California 95616

Received August 9, 1993[⊛]

Abstract: Resonance Raman (RR) spectra are reported for ferrous yeast iso-1 cytochrome *c* and its *meso*-d_4, pyrrole-^{15}N, 2,4-di(a-d_1), and 2,4-di(b-d_2) isotopomers, obtained by the enzymatic coupling of apoprotein with labeled hemes. Three excitation wavelengths, in resonance with the B (413.1 nm) and Q (520.8 and 530.9 nm) states, were used to selectively examine vibrational modes of different symmetry. On the basis of the observed isotope shifts and the measured depolarization ratios and by analogy to those of nickel octaethylporphyrin, RR bands are assigned to nearly all of the porphyrin in-plane and many of the out-of-plane skeletal modes. Assignments of the 2,4-thioether substituent modes are secured from their isotope shifts upon selective deuteration; the C–S stretching bands of these substituents are among the strongest bands in the B-resonant spectrum. Candidate bands are also found for modes of the methyl and propionate substituent groups. The characteristic four sets of doublet bands, clustered in the spectral region 330–430 cm^{-1}, are assigned to the porphyrin modes ν_8 and ν_{50} and to pairs of deformation modes of the 2,4-thioether substituents and 6,7-propionate substituents. Out-of-plane distortions of the porphyrin, seen in the high-resolution X-ray crystal structures, are manifested in the RR spectrum in the following ways: (1) two anomalously polarized bands (ν_{19} and ν_{21}) gain substantial intensity in the B-state excited spectrum, and a depolarized band (ν_{15}) is extraordinarily strong; (2) many IR-active E_u modes become RR-active, and some of them split into doublets; (3) out-of-plane deformation modes involving methine wagging, pyrrole folding, and pyrrole swiveling coordinates are activated, and two E_g modes (γ_{20} and γ_{21}) are split. Band frequencies are almost the same for ferric as ferrous cytochrome *c*, except for the high-frequency skeletal modes, which reflect the different extent of back-bonding. The relative intensities are also very similar, reflecting the minimal change in heme structure in the two oxidation states.

Introduction

Resonance Raman (RR) spectroscopy has been extensively applied to the study of structure, dynamics, and reaction mechanisms in heme proteins,[1] since the first investigation of cytochrome *c* RR spectra some 20 years ago.[2] Raman enhancement via resonance with the porphyrin π–π^* transitions selectively reveals the vibrational modes of the chromophore without interference from the protein matrix. Through extensive studies of heme proteins and model compounds, marker bands of the porphyrin core size and of electron density in the porphyrin π and π^* orbitals have been discovered among the high-frequency (1350–1650 cm^{-1}) skeletal modes.[3] These are very useful in establishing oxidation, spin, and ligation states of the heme.

Heme protein RR spectra are very rich in the mid- (1350–900 cm^{-1}) and low- (900–100 cm^{-1}) frequency regions and differ substantially from one protein to another.[4] Yet the information contained in these differences has been obscure, because systematic band assignments have been available only in the high-frequency region. A framework for making complete assignments has now been developed through the analysis of the normal modes of nickel octaethylporphyrin (OEP),[5] a compound that models heme proteins in having carbon substituents at all eight pyrrole β-positions of the porphyrin ring and hydrogen atoms at the methine bridges. Almost all of the in-plane as well as the out-of-plane skeletal modes of NiOEP have been assigned, along with most of the internal modes of the ethyl substituents, which give rise to surprisingly strong bands in the RR spectra.[5b] These assignments can be carried over to heme proteins once the alterations associated with the individual substituents, i.e., methyl,[6] propionate, vinyl,[7] and/or formyl,[8] are understood. Because of spectral crowding, however, frequency correspondences alone are inadequate to transfer assignments, and isotopic data are needed.

Cytochrome *c* (cyt *c*) provides a good starting point for a more thorough analysis of heme protein RR spectra because of the continuing interest in the structure of this key electron-transfer protein[9,10] and in its interaction with various redox partner protein

[†] Princeton University.
[‡] University of California, Davis.
[⊛] Abstract published in *Advance ACS Abstracts,* December 1, 1993.

(1) (a) Spiro, T. G., Ed. *Biological Applications of Raman Spectroscopy*; Wiley: New York, 1988; Vol. III. For recent reviews on RR spectroscopy of heme proteins: (b) Abe, M. In *Advances in Spectroscopy*; Clark, R. J. H., Hester, R. E., Eds., Wiley: New York, 1986, Vol. 13, pp 347–393. (c) Kitagawa, T., Ozaki, Y. *Struct. Bonding* **1987**, *64*, 71–114. (d) Spiro, T. G., Czernuszewicz, R. S., Li, X.-Y. *Coord. Chem. Rev.* **1990**, *100*, 541–571. (e) Spiro, T. G.; Smulevich, G.; Su, C. *Biochemistry* **1990**, *29*, 4497–4508. (f) Procyk, A. D.; Bocian, D. F. *Annu. Rev. Phys. Chem.* **1992**, *43*, 465–496.

(2) (a) Spiro, T. G.; Strekas, T. C. *Proc. Nat. Acad. Sci. U.S.A.* **1972**, *69*, 2622–2626. (b) Strekas, T. C.; Spiro, T. G. *Biochim. Biophys. Acta* **1972**, *278*, 188–192.

(3) (a) Spaulding, L. D.; Chang, C. C.; Yu, N.-T.; Felton, R. H. *J. Am. Chem. Soc.* **1975**, *97*, 2517. (b) Parthasarathi, N.; Hansen, C.; Yamaguchi, S.; Spiro, T. G. *J. Am. Chem. Soc.* **1987**, *109*, 3865–3871. (c) Prendergast, K.; Spiro, T. G. *J. Am. Chem. Soc.* **1992**, *114*, 3793–3801.

(4) (a) Desbois, A.; Lutz, M.; Banerjee, R. *Biochemistry* **1979**, *18*, 1510–1518. (b) Babcock, G. T.; Callahan, P. M.; Ondrias, M. R.; Salmeen, I. *Biochemistry* **1981**, *20*, 959–966. (c) Choi, S.; Lee, J. J.; Wei, Y. H.; Spiro, T. G. *J. Am. Chem. Soc.* **1983**, *105*, 3692–3707. (d) Teraoka, J.; Kitagawa, T. *J. Biol. Chem.* **1981**, *256*, 3969–3977.

(5) (a) Abe, M.; Kitagawa, T.; Kyogoku, Y. *J. Chem. Phys.* **1978**, *69*, 4526–4534. (b) Li, X.-Y.; Czernuszewicz, R. S.; Kincaid, J. R.; Stein, P.; Spiro, T. G. *J. Phys. Chem.* **1990**, *94*, 47–61. (c) Li, X.-Y.; Czernuszewicz, R. S.; Kincaid, J. R.; Spiro, T. G. *J. Am. Chem. Soc.* **1989**, *111*, 7012–7023.

(6) Lee, H.; Kitagawa, T.; Abe, M.; Pandey, P. K.; Leung, H.-K.; Smith, K. M. *J. Mol. Struct.* **1986**, *146*, 329–347.

(7) (a) Choi, S.; Spiro, T. G.; Langry, K. C.; Smith, K. M. *J. Am. Chem. Soc.* **1982**, *104*, 4337. (b) Choi, S.; Spiro, T. G.; Langry, K. C.; Smith, K. M.; Budd, L. D.; La Mar, G. N. *J. Am. Chem. Soc.* **1982**, *104*, 4345.

(8) Willems, D. L.; Bocian, D. F. *J. Phys. Chem.* **1985**, *89*, 234–239.

(9) (a) Pettigrew, G. W.; Moore, G. R. *Cytochromes c: Biological Aspects*; Springer-Verlag: Berlin, 1987. (b) Moore, G. R.; Pettigrew, G. W. *Cytochromes c: Evolutionary, Structural and Physicochemical Aspects*, Springer-Verlag: Berlin, 1990.

0002-7863/93/1515-12446$04.00/0

complexes.[11] In addition, its RR spectrum is uncomplicated by the effects of conjugating substituents, since the protoheme vinyl groups are saturated via the formation of covalent thioether links to the side chains of two cysteine residues. Consequently, NiOEP is a better model for cyt *c* than for most heme proteins, in which the protoheme vinyl groups are not saturated. At the same time, the RR spectra are extremely rich, especially in the low-frequency region.[12] This richness is associated with heme protein interactions in the native structure, since denaturation of cyt *c* or conversion to the A state, in which secondary but not tertiary structure is maintained, collapses many of the bands.[13] The high-resolution crystal structure reveals a pronounced saddling distortion of the heme group,[10] which our study shows to be the source of much of the RR band activation.

Isotopic labeling of the heme can be accomplished for many heme proteins by simple extraction and reconstitution procedures.[14] This approach is precluded for cyt *c* because the heme moiety in cyt *c* is covalently attached to the polypeptide chain through two stereospecific thioether bonds at the 2 and 4 positions. These two bonds do not form spontaneously. We have therefore developed enzymatic methodology to couple the apocyt *c* with labeled hemes based on cytochrome *c* heme lyase. Using this procedure, we have labeled the heme in cyt *c* with ^{15}N and with deuterium at the methine bridges (*meso*-d_4) and the C_a and C_b atoms of the 2 and 4 thioether substituents. The isotope shift pattern together with selective wavelength excitation and polarization measurements have allowed us to assign over 70 vibrational modes, including almost all of the in-plane skeletal modes, many of the out-of-plane modes, and most of the substituent modes. It is expected that the reconstitution procedure will also further other spectroscopic studies (e.g., NMR) of cyt *c* through the use of specific isotope labels on the heme.

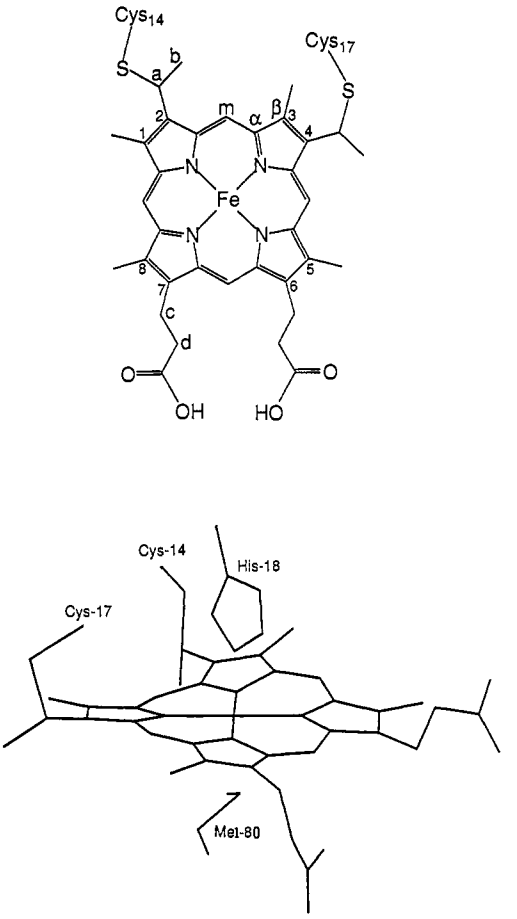

Figure 1. Atom labeling scheme of the heme moiety in cytochrome *c*, together with a structural diagram showing the saddling distortion in the native protein.

Experimental Section

Materials. The following materials were purchased from Sigma: yeast iso-1 cyt *c*, cyt *c* oxidase, lactate dehydrogenase (cyt b_2), and hemin. All the heme isotopomers were synthesized according to published procedures.[15]

Preparation of Apocyt *c*. Yeast iso-1 cyt *c* was purified according to the procedures described by Basile et al.[16] The heme was cleaved from the holoprotein by the method of Fisher et al.[17] with the following modification: 200 mg of cyt *c*, dissolved in a minimum amount of deionized water, was added to 15 mL of solution (pH 2.0) containing 8 M urea, 0.1 M NaCl, and 1.2 g of mercuric chloride, the pH being adjusted with hydrochloric acid. After incubation at 40 °C for 4 h, the mixture was passed over a 2 × 80-cm Sephadex G-25 chromatographic column, which had previously been equilibrated with 0.1 N acetic acid. The lyophilized white powder of apocyt *c* was dissolved in 0.1 M potassium phosphate buffer (pH 7.0) containing 0.2 M β-mercaptoethanol. The solution of 200 μM apocyt *c* was divided into 2-mL aliquots and stored under liquid nitrogen until ready for use.

Isolation of Mitochondria. Yeast mitochondria were isolated from commercial baker's yeast (Red Star) using a modification of Tzagoloff's procedure.[18] The homogenized white powder of frozen yeast (2 lb) was suspended in 1.2 L of 50 mM potassium phosphate buffer (pH 7.0) and allowed to thaw at room temperature. The suspension was then homogenized again with a Waring blender at low speed for 20 s and centrifuged at 3000*g* for 1 h. The supernatant was decanted and retained, while the precipitated whole cells and cell debris were discarded. After centrifugation at 9000*g* for 90 min, the supernatant was decanted and the sedimented mitochondrial pellet was suspended in cold 50 mM potassium phosphate buffer (pH 7.0) to about 15 mg protein/mL.

Solubilization and Partial Purification of Cytochrome *c* Heme Lyase. Mitochondrial proteins were solubilized at 0 °C by treating the mitochondrial suspension with 10% Triton X-100 to make the final concentration of detergent 1%. The solution was then stirred at 0 °C for 40 min and centrifuged at 20 000*g* for 30 min. The supernatant was removed and treated with CP Sephadex C-25 (Pharmacia) twice for a total of 40 min. After removal of the resin, the solution was divided into 40-mL aliquots and stored at −80 °C until ready for use. No loss of enzymatic activity was noticed over a period of 12 months.

Reconstitution of Cyt *c*. Holocytochrome *c* was reconstituted by incubating overnight 20 mL of cytochrome *c* heme lyase preparation, containing 10 mg of protein/mL, 15 μM apocyt *c*, and 100 μM heme. The reaction was started by anaerobically adding excess sodium dithionite. The mixture was then passed over a 2.5- × 80-cm Sephadex G-25 column, which had been previously equilibrated with 20 mM potassium phosphate buffer (pH 7.0) and layered with 1.0 mL of 0.5 M potassium ferricyanide. The pink eluent was loaded onto a small CP Sephadex C-25 column (bed volume 4 mL). The reddish cyt *c* was adsorbed on the top of the resin.

(10) (a) Dickerson, R. E.; Kopka, M. L.; Borders, C. L., Jr.; Varnum, J. C.; Weinzierl, J. E.; Margoliash, E. *J. Mol. Biol.* **1967**, *29*, 77–95. (b) Dickerson, R. E.; Kopka, M. L.; Weinzierl, J. E.; Varnum, J. C.; Eisenberg, D.; Margoliash, E. *J. Biol. Chem.* **1967**, *242*, 3015–3018. (c) Takano, T.; Kallai, O. B.; Swanson, R.; Dickerson, R. E. *J. Biol. Chem.* **1973**, *248*, 5234–5255. (d) Takano, T.; Dickerson, R. E. *J. Mol. Biol.* **1981**, *153*, 79–94. (e) Takano, T.; Dickerson, R. E. *J. Mol. Biol.* **1981**, *153*, 95–115. (f) Louie, G.; Brayer, G. D. *J. Mol. Biol.* **1990**, *214*, 527–555. (g) Berghuis, A. M.; Brayer, G. D. *J. Mol. Biol.* **1992**, *223*, 959–976.

(11) (a) McLendon, G. *Acc. Chem. Res.* **1988**, *21*, 160–167. (b) Mauk, A. G. *Struct. Bonding* **1991**, *75*, 131–157. (c) Hildebrandt, P.; Heimburg, T.; Marsh, D.; Powell, G. L. *Biochemistry* **1990**, *29*, 1661–1668. (d) Hildebrandt, P.; English, A. M.; Smulevich, G. *Biochemistry* **1992**, *31*, 2384–2392. (e) Zhou, C.; Ye, S.; Kim, J. H.; Cotton, T. M.; Yu, X.; Lu, T.; Dong, S. *J. Electroanal. Chem. Interfacial Electrochem.* **1991**, *319*, 71–83

(12) Yu, N.-T.; Srivastava, R. B. *J. Raman Spectrosc.* **1980**, *9*, 166–171.

(13) Jordan, T.; Austin, J; Spiro, T. G., to be submitted.

(14) Teale, F. W. J. *Biochim. Biophys. Acta* **1959**, *35*, 543. (b) Sano, Y. In *The Porphyrins*; Dolphin, D., Ed.; Academic Press: New York, 1979; Vol. VII, pp 377–402.

(15) (a) Kenner, G. W.; Smith, K. M.; Sutton, M. J. *Tetrahedron Lett.* **1973**, 1303–1306. (b) Budd, D. L.; La Mar, G. N.; Langry, K. C.; Smith, K. M.; Nayyir-Mazhir, R. *J. Am. Chem. Soc.* **1979**, *101*, 6091–6096. (c) Smith, K. M.; Morris, I. K. *J. Chem. Res. (S)*, **1988**, 16–17.

(16) Basile, G.; Bello, C. D.; Taniuchi, H. *J. Biol. Chem.* **1980**, *255*, 7181–7191.

(17) Fisher, W. R.; Taniuchi, H.; Anfinsen, C. B. *J. Biol. Chem.* **1973**, *248*, 3188–3195.

(18) Tzagoloff, A. *J. Biol. Chem.* **1969**, *244*, 5020–5026.

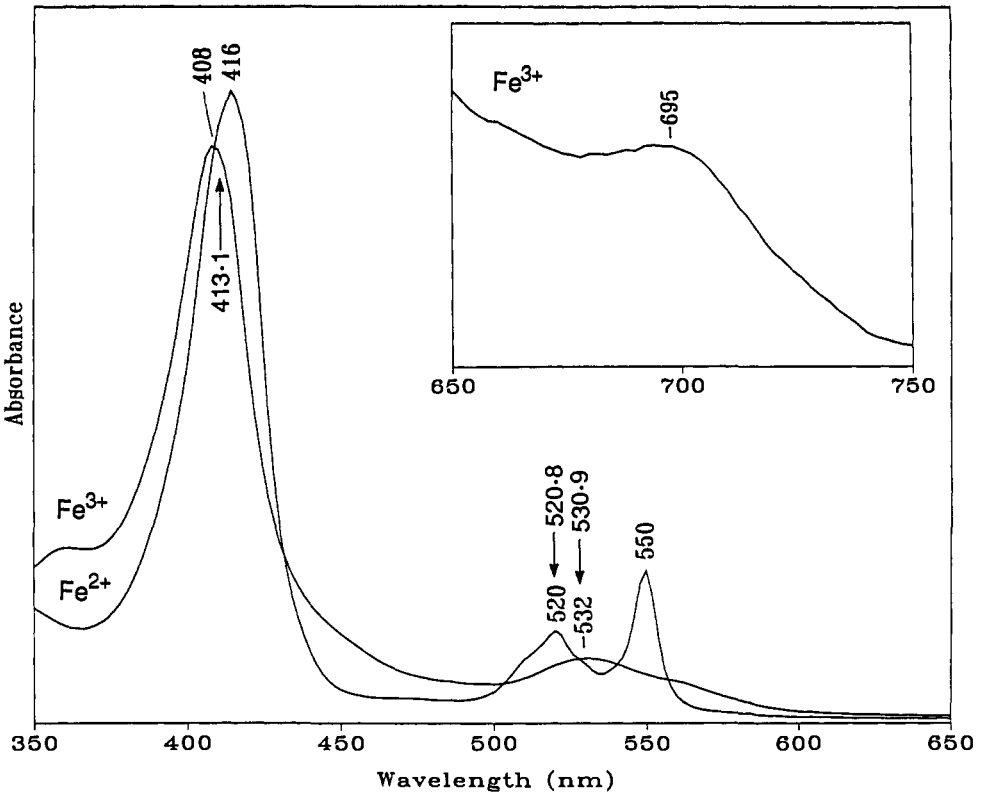

Figure 2. Electronic absorption spectra of *meso*-d_4 yeast iso-1 cytochrome *c* in ferric and ferrous states. The insert shows the 695-nm band of the ferric cytochrome *c*, while the arrows indicate the position of resonance Raman excitation lines. The reconstituted protein sample was dissolved in 50 mM potassium phosphate buffer, pH 7.0. Ferrous cytochrome *c* was prepared by adding 5-fold ascorbic acid.

After the column had been washed with 100 mL of 50 mM potassium phosphate buffer at pH 7.0, cyt *c* was eluted with the same buffer containing 0.5 M KCl. Typically, 35 nmol (0.5 mg based on a molecular weight of 12 300) of ferric cyt *c* was isolated.

Spectroscopic Measurements. UV–visible absorption spectra were recorded at 25 °C with a Hewlet-Packard 8452A spectrophotometer. RR spectra were acquired on a Spex 1403 scanning double monochromator under the control of an IBM-AT computer. Excitation lines (413.1, 520.8, and 530.9 nm) were provided by an Innova K100 Kr^+ laser (Coherent). Samples were positioned in a backscattering geometry and cooled to a nominal temperature of 12 K on a copper tip with a Displex helium closed-cycle refrigerator (Air Products). All the spectral data were imported into and processed with Labcalc software (Galactic Industries Corp.).

Results

1. Reconstitution of Cyt *c*. Figure 1 shows the molecular structure of the heme moiety in cyt *c*. The two vinyl groups of protoheme become saturated by the formation of two thioether linkages with two cysteine residues of apoprotein. Because of these covalent bonds, the conventional method used to reconstitute many heme proteins by simply mixing the heme with the apoproteins is precluded for cyt *c*. Sano and Tanaka[19] did obtain a cyt *c*-like species by combining apocyt *c* with protoporphyrinogen, followed by iron insertion. The product was not fully characterized, however, and the addition reaction of the SH group to the vinyl groups is not expected to yield stereospecific linkages.

Stereospecificity can be assured, however, by enzymatic coupling using cytochrome *c* heme lyase. This enzyme has not been isolated and purified because of its low abundance and lability. But enzymatic activity has been detected in mitochondria by a number of groups.[20] Taniuchi and co-workers solubilized the enzyme using Triton X-100 and concentrated it by ammonium sulfate fractionation.[20d] They also demonstrated the use of this enzyme preparation to obtain holocytochrome *c* and studied its substrate specificity.[20e,f] Seeking to adapt Taniuchi's procedure to the reconstitution of cyt *c*, we found that the crude heme lyase preparation is invariably contaminated with endogenous cyt *c*. In addition, the enzymatic method used to isolate yeast mitochondria in previous work[20d,k] is not applicable to large-scale preparation. Therefore, we have adopted Tzagoloff's procedure to obtain larger quantities of yeast mitochondria and developed an efficient chromatographic method to remove the endogenous cyt *c* from the enzyme preparation. Our treatment of the crude solubilized enzyme with CP Sephadex C-25 ion exchanger yields a partially purified form of cytochrome *c* heme lyase that is essentially depleted of endogenous cyt *c*. This treatment also facilitates isolation of the reconstituted cyt *c* by removing other contaminating proteins which bind to the ion-exchange resin. Further purification of the reconstituted protein was not needed.

The biological activity of reconstituted cyt *c* was tested with each of its enzymatic redox partners. The oxidation rate of ferrous protein by cyt *c* oxidase[21b] and the reduction rate of ferric protein by lactate dehydrogenase (cyt b_2) with L-(+)-lactic acid[21a] were nearly the same for reconstituted and native cyt *c*. Moreover, the

(19) Sano, S.; Tanaka, K. *J. Biol. Chem.* **1964**, *230*, PC3109–PC3110.

(20) (a) Korb, H.; Neupert, W. *Eur. J. Biochem.* **1978**, *91*, 609–620. (b) Zimmermann, R.; Paluch, U.; Neupert, W. *FEBS Lett.* **1979**, *108*, 141–146. (c) Hennig, B.; Neupert, W. *Eur. J. Biochem.* **1981**, *121*, 203–212. (d) Taniuchi, H.; Basile G.; Taniuchi, M.; Veloso, D. *J. Biol. Chem.* **1983**, *258*, 10963–10966. (e) Veloso, D.; Juillerat, M.; Taniuchi, H. *J. Biol. Chem.* **1984**, *259*, 6067–6073. (f) Visco, C.; Taniuchi, H.; Berlett, B. S. *J. Biol. Chem.* **1985**, *260*, 6133–6138. (g) Nicholson, D. W.; Kohler, H.; Neupert, W. *Eur. J. Biochem.* **1987**, *164*, 147–157. (h) Dumont, M. E.; Ernst, J. F.; Hampsey, D. M.; Sherman, F. *EMBO J.* **1987**, *6*, 235–241. (i) Nicholson, D. W.; Hergersberg, C.; Neupert, W. *J. Biol. Chem.* **1988**, *263*, 19034–19042. (j) Dumont, M. E.; Ernst, J. F.; Hampsey, D. M.; Sherman, F. *J. Biol. Chem.* **1988**, *263*, 15928–15937. (k) Nicholson, D. W.; Neupert, W. *Proc. Natl. Acad. Sci. U.S.A.* **1989**, *86*, 4340–4344. (l) Gonzales, D. H.; Neupert, W. *J. Bioenerg. Biomembr.* **1990**, *22*, 753–768. (m) Hakvoort, T. B. M.; Sprinkle, J. R.; Margoliash, E. *Proc. Natl. Acad. Sci. U.S.A.* **1990**, *87*, 4996–5000. (n) Stuart, R. A.; Nicholson, D. W.; Wienhues, U.; Neupert, W. *J. Biol. Chem.* **1990**, *265*, 20210–20219.

(21) (a) Morton, R. K.; Sturtevant, J. M. *J. Biol. Chem.* **1964**, *239*, 1614–1624. (b) Errede, B. J.; Kamen, M. D. *Biochemistry* **1978**, *17*, 1015–1027.

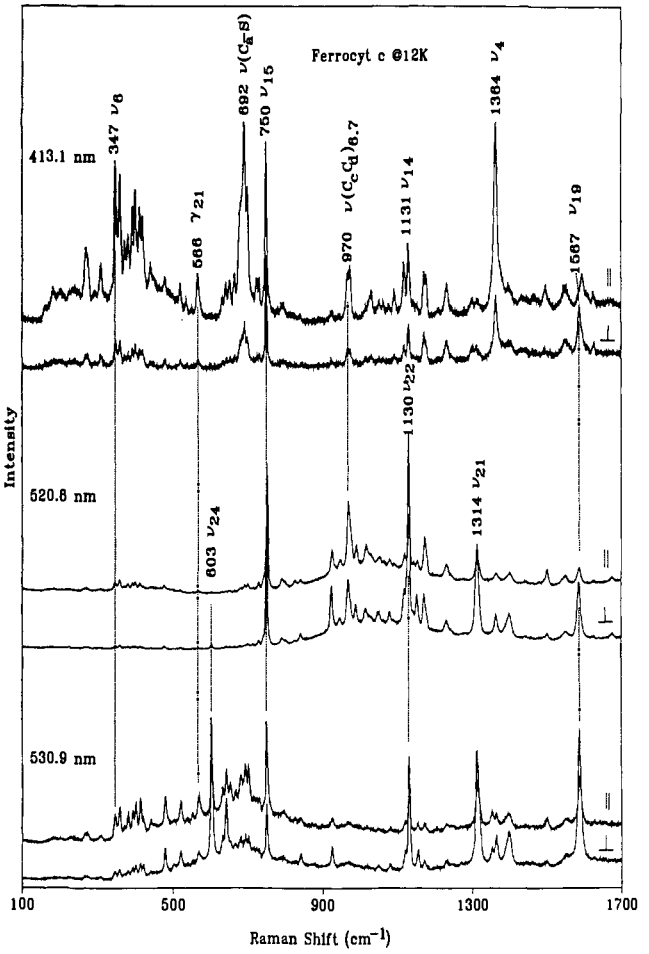

Figure 3. Overview of the resonance Raman spectra of ferrous cytochrome *c* at 12 K, obtained with both B- (413.1 nm) and Q-state excitations (520.8 and 530.9 nm).

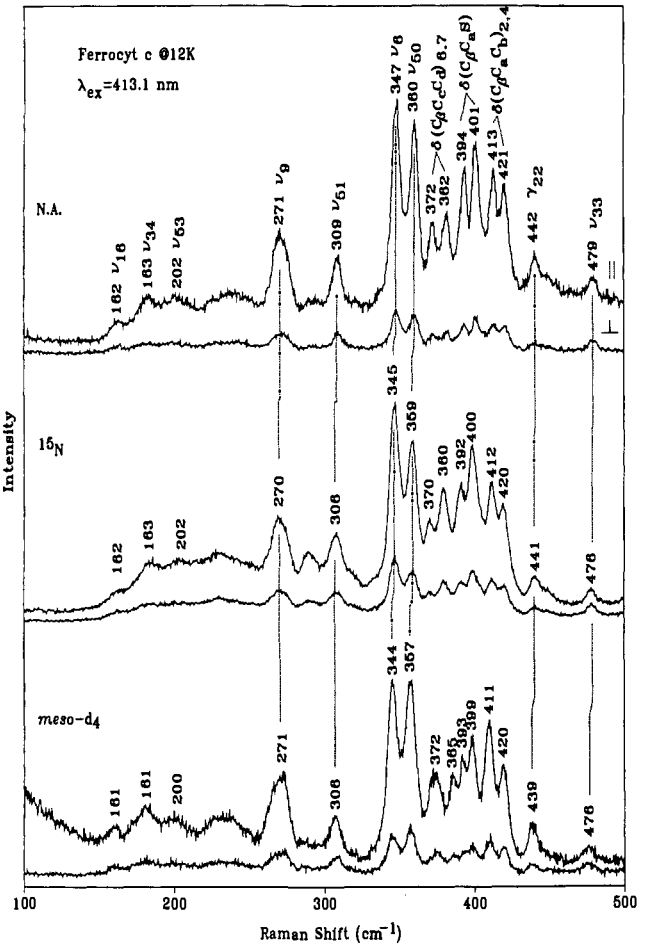

Figure 4. 413.1-nm excited resonance Raman spectra (100–500 cm^{-1}) of natural abundance (N.A.), *meso*-d_4, and pyrrole-^{15}N ferrous cytochrome *c* at 12 K.

electronic absorption spectra in both the ferric and ferrous forms, shown in Figure 2, are the same for reconstituted and native proteins. In particular, the 695-nm band of the ferric protein, which is diagnostic for the coordination of methionine to heme iron,[22] is fully developed in the reconstituted protein.

2. RR Spectra of Cyt *c* and Its Isotopomers. Figure 3 presents an overview of the RR spectra of ferrous yeast iso-1 cyt *c* with three excitation lines, at 413.1, 520.8, and 530.9 nm, in resonance with the B and Q electronic transitions of the heme. The samples were cooled to low temperature (12 K) to achieve higher resolution than is attainable at room temperature and to eliminate the broad, sloping background from the incoherently broadened resonance fluorescence associated with Q-band excitation.[23] The low temperature, together with the small spectral band pass (4 cm^{-1}) of the spectrometer, yielded spectra in which many closely spaced Raman bands can be resolved. Although the frozen solution scrambles the laser polarization to some extent, the observed depolarization ratios are nevertheless sufficient to differentiate anomalously polarized (ap), polarized (p), and depolarized (dp) modes.

Figures 4–7 compare the RR spectra obtained with B-state (413.1 nm) excitation for natural abundance ferrous cyt c and its pyrrole-^{15}N and *meso*-d_4 heme reconstituted derivatives, while those obtained with the Q_1- (520.8 nm) and Q_0-state (530.9 nm) excitations are shown in Figures 8–11. The experimental details for each spectrum are given in the figure legends. Corresponding modes for the isotopomers, as judged from their intensity pattern and expected isotope shifts, are correlated with dotted lines. Mode assignments, which are indicated in the figures and listed in Table I, were made with reference to the normal mode description of NiOEP on the basis of the depolarization ratios and isotope shifts.[5b]

The *meso*-d_4 spectrum reveals the absence of any detectable endogenous cyt *c* in our reconstituted product. No underlying unshifted bands can be seen. We note in particular the complete disappearance of the band seen at 1231 cm^{-1} in the natural abundance spectrum (Figure 6). This mode is assigned to the skeletal mode ν_{13}, involving mainly the C_m–H in-plane bending vibration.[5b] Deuteration of the *meso* protons is expected to shift this mode out of the spectral region. Similarly, a clean shift is observed for the ν_{15} band at 750 cm^{-1} (Figure 5). Thus, our procedure yields isotopically pure protein, facilitating the detection of even subtle isotopic effects on the spectrum.

Figures 12–16 show the effects of selective isotope substitution of the 2,4-substituents in cyt *c* on the RR spectra. The large isotope shifts of some bands reveal the contribution from the internal vibrations of the 2,4-substituents, which are correlated in the figures with dotted lines. Modes of methyl and propionic acid substituents, which are also marked in the figures, are suggested from their insensitivity to isotope substitution, both in the skeletal (*meso*-d_4 and ^{15}N) and 2,4-substituent positions, and also from their frequency correspondences with spectra of NiOEP[5] and nickel(II) etioporphyrin-I,[24] for which the methyl and methylene modes have been secured from their isotope shifts.

Figures 17 and 18 contain RR spectra of ferric cyt *c* and of its ^{15}N and *meso*-d_4 isotopomers. Because ferric cyt *c* undergoes photoinduced reduction at 12 K, these spectra were obtained

(22) Sherman, F.; Taber, H.; Campbell, W. *J. Mol. Biol.* **1965**, *13*, 21–39.
(23) Friedman, J. M.; Rousseau, D. L. *Chem. Phys. Lett.* **1978**, *55*, 488–492.
(24) Hu, S.; Spiro, T. G., to be published.

Table I. Resonance Raman Frequencies and Their Normal Mode Assignments of Ferrous Cytochrome *c* and Its Isotopomers

	N.A.[a]	Δ(^{15}N)	*meso*-d_4	2,4-di(a-d_1)	2,4-di(b-d_2)	assignment, N.A.–NiOEP, Δ(^{15}N), *meso*-d_4		N.A.[a]	Δ(^{15}N)	*meso*-d_4	2,4-di(a-d_1)	2,4-di(b-d_2)	assignment, N.A.–NiOEP, Δ(^{15}N), *meso*-d_4
dp[b]	1626	0	1609	1625	1626	ν_{10} 1655 (0), 1645	ap	925	2	926	932	921	ν_{46}
dp	1610	1		1608	1609	ν_{38} 1604 (0), 1604	ap	842	0	576			γ_{19} 841 (0), [773]
p[c]	1596	3	1592	1594	1595	ν_2 1602 (1), 1601	p	841	0				γ_{10} 853 (0), [501]
ap[d]	1587	0	1573	1587	1587	ν_{19} 1603 (1), 1581	p	826	0				γ_4 844 (0), 681
dp	1551	2	1546	1549	1550	ν_{11} 1577 (1), 1576	p	796	7		782	791	ν_6 804 (5), 799
p	1501	8	1372	1501	1501	$2\nu_{15}$	dp	750	4	685	750	750	ν_{15} 751 (3), 683
p	1496	1	1489	1495	1496	ν_3 1520 (1), 1512	p	729	5	725	728	727	γ_5 739 (6), 760
dp	1403	0	1403	1400	1401	ν_{29} 1407 (1), 1405	p	724	4	716	719	717	γ_{11} 732 (0), [790]
ap	1400	3	1397	1400	1400	ν_{20} 1393 (0), 1393	p	700	6	699	700	700	ν_7 674 (3), 668
p	1364	7	1363	1364	1364	ν_4 1383 (7), 1382	p	692	0	685	689	687	ν(C_aS)
dp	1354	4		1254	1352	$\nu_{15} + \nu_{24}$	p	682	1	677	678	677	ν(C_aS)
dp			1337			ν_{12} [1330] [6], 1331	p	666	1	654	661	653	γ_{20} [731] [0], [712]
dp	1317	6		906	1283	$\delta(C_aH)_{2,4}$	p	653	1		647	647	γ_{20}
ap	1314	3	891	1312	1312	ν_{21} 1307 (4), 887	p	642	2	640			ν_{48} 605 (0), 600
dp	1302	2		906	1268	$\delta(C_aH)_{2,4}$	p	633	0	630	631	629	ν_{48}
dp	1232	2	952	1240	1230	ν_{13} 1220 (2), 948	ap	603	0	601	603	602	ν_{24} 597 (1), 582
p	1211	3				ν_{42} 1231 (3), 948	p	568	1	550	568	567	γ_{21} 656 (0), [627]
dp	1180	5		1177	1178		dp	552		542	551	551	γ_{21}
dp	1174	9	1172	1172	1171	ν_{30} 1159 (10), 1159	p	536	1		535	535	ν_{49} 544 (0), 543
p	1154	6		1155	1153	ν_{43} 1153 (8), 1185	dp	520	1	517	520	520	γ_{12} 612 (0), 652
p	1144	8			1144	ν_{43}	ap	502	0	517	500	501	ν_{25} 551 (0), 545
dp	1131	13		1130	1131	ν_{14} 1131 (12), 1186	dp	479	1	476	473	476	ν_{33} 493 (1), 490
ap	1130	13	1221	1133	1131	ν_{22} 1121 (15), 1202	p	442	1	439	440	439	γ_{22} 494 (2), 483
p	1119	8	1120	1103	1118	ν_5 1138 (7), 1138	p	421	1	420	420	410	$\delta(C_\beta C_a C_b)_{2,4}$
ap	1119	9	1147	1122	1126	ν_{44} 1133 (12), 1151	p	413	1	411	412	410	$\delta(C_\beta C_a C_b)_{2,4}$
p	1093	3				$\delta(C_bH_3)_{2,4}$	p	401	1	399	400	398	$\delta(C_\beta C_a S)$
ap	1080	1	1090	1085	1084	ν_{23} 1058 (0), 1058	p	394	2	393	394	398	$\delta(C_\beta C_a S)$
p	1078	0		1080	1084	$\delta(CH_3)$	p	382	2	385	381	382	$\delta(C_\beta C_c C_d)_{6,7}$
p	1063	0		1064	1065	$\delta(CH_3)$	p	372	2	372	372	371	$\delta(C_\beta C_c C_d)_{6,7}$
p	1053	3		1038		$\delta(C_bH_3)_{2,4}$	p	360	1	357	359	360	ν_{50} [358] [1], [357]
ap	1050	1	1052	1064	861/874	$\delta(C_bH_3)_{2,4}$	p	347	2	345	347	347	ν_8 360/343 (2/1), 353/343
dp	1032	10		1029	1026	ν_{31} 1015 (9), 1003							
dp	1016	4		1188/1203	932/939	$\nu(C_aC_b)_{2,4}$	p	309	1	308	307	308	ν_{51} 328 (0), 322
dp	990	6	982	989		ν_{45} 996(5), 995	p	271	1	271	270	269	ν_9 263/274 (2/1), 262/274
p	975	2	972	969	971	$\nu(C_cC_d)_{6,7}$							
p	969	3	972			$\nu(C_cC_d)_{6,7}$	p	202	0	200	200	199	ν_{53} 212 (0), 212
dp	947	6	935	951	951	ν_{32} 938 (0), 934	p	183	0	181	181	179	ν_{34} 197 (0), 197
dp	925	2		932	921	ν_{46} 927 (3), 919	p	162	0	161	162	159	ν_{18} 168 (0), 168

[a] N.A., natural abundance. [b] dp, depolarized mode. [c] p, polarized mode. [d] ap, anomalously polarized mode.

only for room temperature samples contained in spinning NMR tubes with 413.1-nm excitation but nevertheless permit a careful comparison with ferrous cyt *c*.

Discussion

A. In-Plane Skeletal Vibrations. The high-frequency skeletal modes, above 1350 cm^{-1}, are well-understood and have been discussed many times with respect to oxidation and spin-state sensitivity.[25] Below the intense ν_4 band, assignments of the cyt *c* skeletal modes have been uncertain because of spectral congestion. The isotope data reveal the sources of this congestion: activation of substituent modes, of porphyrin out-of-plane modes, and also of in-plane skeletal modes which have E_u symmetry for the idealized D_{4h} point group of the heme chromophore. These E_u modes do not appear in RR spectra of the NiOEP reference compound, but they have been analyzed via the IR spectrum, and the isotope shift pattern leaves little doubt about their assignment in the cyt *c* RR spectra. As seen in Table II, activation is observed for 11 out of the 18 E_u modes, and in two cases, ν_{43} and ν_{48}, pairs of bands are observed, indicating a splitting of the E_u degeneracy. The activation and splitting are attributed to protein-induced heme distortions, as discussed below.

The deuteration of *meso* hydrogens produces a complex isotope shift pattern of the RR bands between 900 and 1300 cm^{-1}, because of the vibrational coupling of $\delta(C_m–H)$ with other local coordinates in this region (Table II). Firm assignments of these drastically shifted bands are difficult in the absence of experimental data from the doubly-labeled *meso*-d_4 and ^{15}N isotopomer but can be tentatively made by analogy to those of NiOEP.[5] Thus, the downshifted $\delta(C_m–D)$ modes are assigned to spectral features at 891 (ν_{21}), 952 (ν_{13}), and 945 (ν_{42}) cm^{-1}. The expected upshifts, caused by the relief of vibrational coupling with $\delta(C_m–H)$ coordinate, are observed for modes immediately below those of $\delta(C_m–H)$, i.e., ν_{22} (1221 from 1130 cm^{-1}), ν_{43} (1205 from 1154 cm^{-1}), and ν_{44} (1147 from 1119 cm^{-1}).

Near 700 cm^{-1}, there are three well-resolved bands (682, 692, and 700 cm^{-1}) (Figures 5 and 10). The 700 cm^{-1} feature shows the pyrrole-^{15}N shift (6 cm^{-1}), expected for ν_7, but the other two bands are ^{15}N-insensitive. They are assigned to the $\nu(C_a–S)$ stretching modes from their isotope shifts upon selective deuteration of the 2,4-substituents (*vide infra*).

(25) For a review, see: (a) Cartling, B. In *Biological Applications of Raman Spectroscopy*; Spiro, T. G., Ed.; Wiley: New York, 1988; Vol. III, pp 217–248. (b) Strekas, T. C.; Spiro, T. G. *Biochim. Biophys. Acta* **1974**, *351*, 237–245. (c) Kitagawa, T.; Ozaki, Y.; Teraoka, J.; Kyogoku, Y.; Yamanaka,T. *Biochim. Biophys. Acta* **1977**, *494*, 100–114. (d) Kitagawa, T.; Ozaki, Y.; Kyogoku, Y.; Horio, T. *Biochim. Biophys. Acta* **1977**, *495*, 1–11. (e) Forster, M.; Hester, R. E.; Cartling, B.; Wilbrandt, R. *Biophys. J.* **1982**, *38*, 111–116. (f) Cartling, B. *Biophys. J.* **1983**, *43*, 191–205. (g) Myer, Y. P.; Srivastava, R. B.; Kumar, S.; Raghavendra, K. *J. Protein Chem.* **1983**, *2*, 13–42. (h) Uno, T.; Nishimura, Y.; Tsuboi, M. *Biochemistry* **1984**, *23*, 6802–6808. (i) Hildebrandt, P.; Stockburger, M. *J. Phys. Chem.* **1986**, *90*, 6017–6024. (j) Verma, A. L.; Kimura, K.; Nakamura, A.; Yagi, T.; Inokuchi,H.; Kitagawa, T. *J. Am. Chem. Soc.* **1988**, *110*, 6617–6623. (k) Hildebrandt, P.; Stockburger, M. *Biochemistry* **1989**, *28*, 6722–6728. (l) Hildebrandt, P.; Stockburger, M. *Biochemistry* **1989**, *28*, 6710–6721. (m) Larsen, R. W.; Chavez, M. D.; Nunez, D. J.; Davidson, M. W.; Knaff, D. B.; Krulwich, T. A.; Ondrias, M. R. *Arch. Biochem. Biophys.* **1990**, *283*, 266–270. (n) Hildebrandt, P. *Biochim. Biophys. Acta* **1990**, *1040*, 175–186. (o) Hildebrandt, P.; Pielak, G. J.; Williams, R. J. P. *Eur. J. Biochem.* **1991**, *201*, 211–216 (p) Heibel, G.; Griebenow, K.; Hildebrandt, P. *Biochim. Biophys. Acta* **1991**, *1060*, 196–202. (q) Heimburg, T.; Hildebrandt, P.; Marsh, D. *Biochemistry* **1991**, *30*, 9084–9089.

Table II. Allocation of the Observed In-Plane Skeletal Frequencies of Ferrous Cytochrome *c* to the Local Coordinates[a]

local coordinate[b]	A_{1g}	B_{1g}	A_{2g}	B_{2g}	E_u
$\nu(C_mH)$	ν_1 [3041]			ν_{27} [3041]	ν_{36} [3040]
$\nu(C_\alpha C_m)_{asym}$		ν_{10} 1626 *1655*	ν_{19} 1587 *1603*		ν_{37} *[1637]*
$\nu(C_\beta C_\beta)$	ν_2 1596 *1602*	ν_{11} 1551 *1577*			ν_{38} 1610 *1604*
$\nu(C_\alpha C_m)_{sym}$	ν_3 1496 *1520*			ν_{28} *1483*	ν_{39} *1501*
ν(pyr quarter-ring)			ν_{20} 1400 *1393*	ν_{29} 1403 *1407*	ν_{40} *1396*
ν(pyr half-ring)$_{sym}$	ν_4 1364 *1384*	ν_{12} *1343*			ν_{41} *[1346]*
$\delta(C_mH)$		ν_{13} 1232 *1220*	ν_{21} 1314 *1307*		ν_{42} 1211 *1231*
$\nu(C_\beta C_1)_{sym}$	ν_5 1119 *1138*	ν_{14} 1131 *1131*			ν_{44} 1119 *1153*
ν(pyr half-ring)$_{sym}$			ν_{22} 1130 *1121*	ν_{30} 1174 *1159*	ν_{43} 1144/1154 *1133*
$\nu(C_\beta C_1)_{asym}$			ν_{23} 1080 *1058*	ν_{31} 1032 *1015*	ν_{45} 990 *996*
δ(pyr deform)$_{asym}$			ν_{24} 603 *597*	ν_{32} 947 *938*	ν_{46} 925 *927*
ν(pyr breathing)	ν_6 796 *804*	ν_{15} 750 *751*			ν_{47} *766*
δ(pyr deform)$_{sym}$	ν_7 700 *674*	ν_{16} *746*			ν_{48} 633/642 *605*
δ(pyr rotat)			ν_{25} 502 *551*	ν_{33} 479 *493*	ν_{49} 538 *544*
ν(NiN)	ν_8 347 *361/343*	ν_{18} 162 *168*			ν_{50} 360 *[358]*
$\delta(C_\beta C_1)_{asym}$					ν_{51} 309 *328*
$\delta(C_\beta C_1)_{sym}$	ν_9 271 *263/274*	ν_{17} *305*	ν_{26} *[243]*	ν_{34} 183 *197*	ν_{52} *263*
δ(pyr transl)				ν_{35} *144*	ν_{53} 202 *212*

[a] The italicized values are those of NiOEP. The bracketed values are the calculated frequencies, for which the experimental values are not available. [b] For the definition of local coordinates of porphyrin in-plane vibrations, see ref 5b.

The ν_8 (347 cm^{-1}) and ν_9 (271 cm^{-1}) modes, which are combinations of metal–N (pyrrole) stretching and pyrrole–substituent bending coordinates, have been shown to be sensitive to the substituent conformations in the case of NiOEP.[5b] Because of structural polymorphism, both the ν_8 and ν_9 modes are doublets for NiOEP in solution. In the cyt *c* spectrum (Figure 4), ν_9 is an isolated band, but there are two ν_8 candidates, 347 and 360 cm^{-1}. Since there is no evidence for structural heterogeneity in the heme pocket of cyt *c* from NMR[26] and X-ray crystal structure studies,[10] two bands for ν_8 are not expected. We therefore assign the two bands to ν_8 (347 cm^{-1}) and ν_{50} (360 cm^{-1}) modes; the latter is one of the E_u modes activated in cyt *c*. Both modes are composed of the same local coordinates but have different phases; their frequencies and isotope shifts are similar. An alternative assignment of the 360-cm^{-1} band to the γ_6 pyrrole tilting out-of-plane mode is excluded, because the *meso*-d_4 and ^{15}N shifts are too small. Hildebrandt[25n] has previously assigned the 360-cm^{-1} band to the ν_{35} overtone, but this assignment can be ruled out because the frequency is much higher than twice the fundamental, which is observed at 144 cm^{-1} and calculated at 151 cm^{-1} for NiOEP.

The ν_8 and ν_{50} bands are the strongest members of a prominent octet of closely spaced bands, from 347 to 421 cm^{-1} (see Figure 3), which are unique to cyt *c* and have been the subject of much speculation. As discussed below, we assign the remaining three pairs of bands to C–C–C and C–C–S bending modes of the propionate and -CH(SR)CH_3 substituents. Quite different assignments have been suggested in earlier studies. Friedman and Hochstrasser[27] proposed that these bands are difference combination bands of higher frequency fundamentals, but this proposal was questioned by Valance and Strekas[28] and is not supported by the present isotope shift data. More recently, Hildebrandt[25n] has suggested overtone and combination assignments for some of the bands ($2\nu_{35}$ for 361.8 cm^{-1}, $2\nu_9$ for 398.2 cm^{-1}, $\nu_{34}+\nu_{35}$ for 413.3 and 419.0 cm^{-1}) and out-of-plane pyrrole-tilting (375 and 382.2 cm^{-1}) for others, but none of these assignments accords with the isotope shift data.

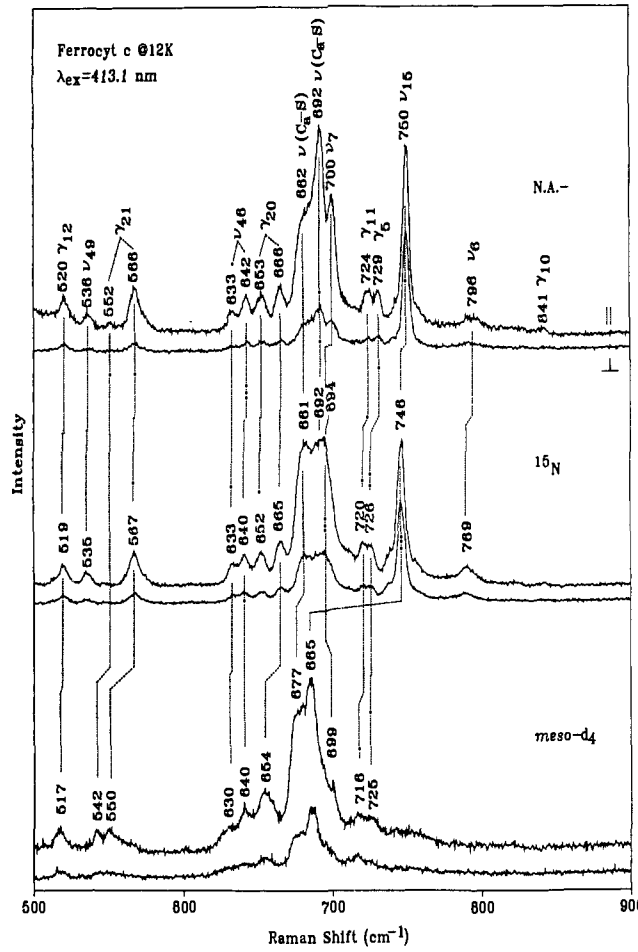

Figure 5. Same as Figure 4, but in the spectral region of 500–900 cm^{-1}.

B. Substituent Modes. The heme group of cyt *c* has three sets of aliphatic peripheral substituents (Figure 1), whose vibrations are expected to appear in the RR spectra, inasmuch as the ethyl modes of NiOEP are found to have significant RR activity.[5b] Assignments are aided by the isotope shifts (Table I) observed for H/D substitution at the C_a or C_b atoms of the vinyl groups in the protoheme used for reconstitution. We note that coordinates for stretching and bending of the porphyrin–substituent bonds are already allocated to the skeletal modes, and are not included among the substituent internal modes.

B1. 2,4-Substituents. The 2,4-substituent group -C_aH(SR)-C_bH_3 has 15 normal vibrational modes, if the SR group is approximated as a point mass. There are four C–H stretching vibrations in the 3000-cm^{-1} region which are not enhanced in the RR spectrum. The remaining 11 vibrations can be divided into S–C_a and C_a–C_b stretching, expected at ~700 and ~1000 cm^{-1} respectively, and deformation modes of the terminal methyl and

(26) (a) Wand, A. J.; DeStefano, D. L.; Feng, Y.; Roder, H.; Englander, S. W. *Biochemistry* **1989**, *28*, 195–203. (b) Feng, Y.; Roder, H.; Englander, S. W. *Biochemistry* **1990**, *29*, 3494–3504. (c) Feng, Y.; Englander, S. W. *Biochemistry* **1990**, *29*, 3505–3509.

(27) (a) Friedman, J. M.; Hochstrasser, R. M. *Chem. Phys.* **1973**, *1*, 457–467. (b) Friedman, J.; Hochstrasser, R. M. *Chem. Phys. Lett.* **1975**, *32*, 414–419. (c) Friedman, J. M.; Hochstrasser, R. M. *J. Am. Chem. Soc.* **1976**, *98*, 4043–4048.

(28) Valance, W. G.; Strekas, T. C. *J. Phys. Chem.* **1982**, *86*, 1804–1808.

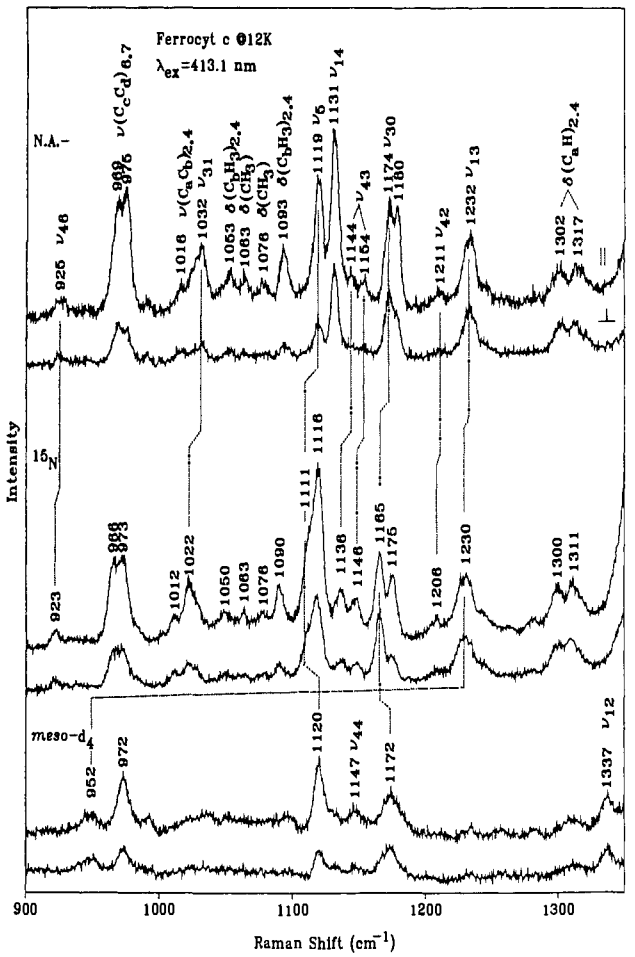

Figure 6. Same as Figure 4, but in the spectral region of 900–1350 cm^{-1}.

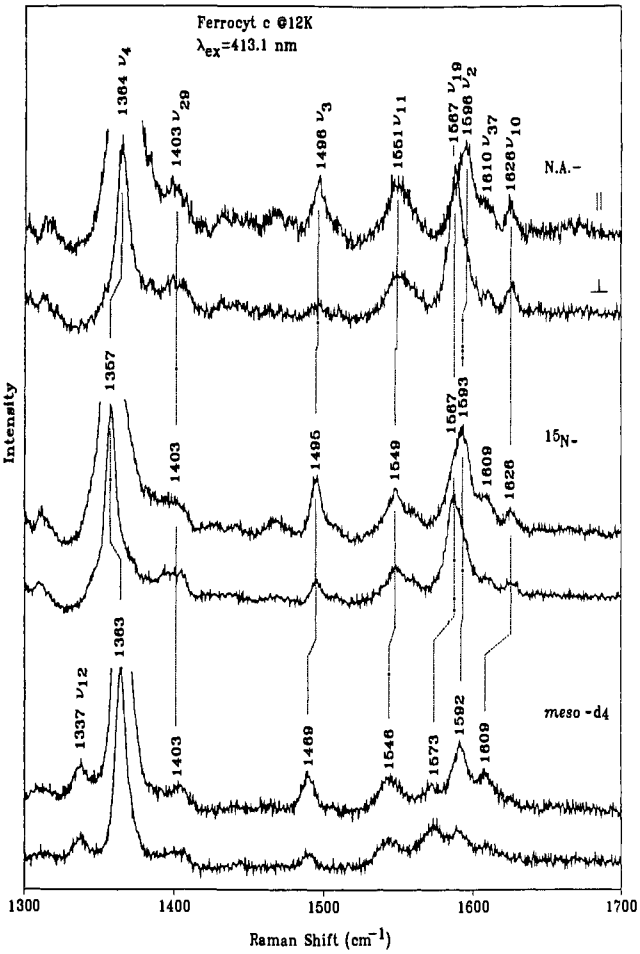

Figure 7. Same as Figure 4, but in the spectral region of 1350–1700 cm^{-1}. For clarity, the parallel trace of the ν_4 band (1364 cm^{-1}) is not shown.

the $C_aH(S)$ groups. For the methyl group, with C_{3v} local symmetry, there are six deformations,[29] including in-phase ($\sim$1380 cm^{-1}) and two degenerate out-of-phase bending modes ($\sim$1460 cm^{-1}), two degenerate rocks (920 to 1000 cm^{-1}), and one torsion ($\sim$200 cm^{-1}). Connecting the terminal C_bH_3 and $C_aH(S)$ groups, there is one C_a–C_b stretching vibration. There remain one C_a–H bending mode (at $\sim$1300 cm^{-1}) and two heavy atom bending modes, involving the C_β–C_a–C_b and C_β–C_a–S bending coordinates, expected near 400 cm^{-1}. There are two $C_aH(S)$-C_bH_3 groups in cyt *c*, and therefore there are two sets of internal vibrations. To a first approximation, corresponding modes of the two substituents have the same frequencies, but their degeneracy may be removed by different interactions of the $C_aH(S)C_bH_3$ group with skeletal vibrations, modulated by their different orientations relative to the porphyrin plane. In addition, within each substituent, the degenerate vibrations of the methyl group (out-of-phase bending and rocking deformations) are split by interactions with the nearby C_a–H bending mode.

C_bH_3 Deformations. There are no candidate RR bands for the C–H bending modes of the terminal methyl groups, but the rocking modes are assigned to bands at 1053 and 1093 cm^{-1} in the 413.1-nm excited spectrum which disappear upon C_a or C_b deuteration (Figure 14). With 530.9-nm excitation (Figure 15), a 1050-cm^{-1} band is shifted up to 1064 cm^{-1} upon C_a deuteration and is shifted down and split into two components at 861 and 876 cm^{-1} upon the C_b deuteration. These bands may represent additional components of the four expected methyl rocking modes of the 2,4-substituent.

$\delta(C_a$–H). The 413.1-nm excited spectrum shows two weak features at 1302 and 1317 cm^{-1} which disappear for C_a deuteration (Figure 14) and are assigned to $\delta(C_a$–H). A new feature at 906 cm^{-1}, assignable to the expected $\delta(C_a$–D) mode, is observed in both the 413.1- and 520.8-nm excited spectra. Deuteration of the methyl group shifts the $\delta(C_a$–H) bands to 1268 and 1283 cm^{-1}.

$\nu(C_a$–$C_b)_{2,4}$. A weak band assignable to C–C stretching is observed at 1016 cm^{-1} in both the 413.1- (Figure 14) and the 520.8-nm excitations (Figure 16). It is upshifted and split into two components at 1188 and 1202 cm^{-1} upon deuteration at C_a. In the 520.8-nm excited spectrum (Figure 16), deuteration of the methyl groups is seen to shift the 1016-cm^{-1} band and split it into components at 932 and 939 cm^{-1}. The isotope shift pattern is reminiscent of those of the ethyl groups in NiOEP.[5b] It is notable, however, that C_a–C_b stretching gives rise to strong bands in the NiOEP spectra, with both B- and Q-band excitation, whereas the enhancement is weak for the 2,4 substituents of cyt *c*.

$\nu(C_a$–S). The thioether linkage connects the apoprotein and the heme moiety; it is important to characterize the C–S stretching vibrations. In a comparative RR study of cyt *c* and cyt b_{562}, Yu and co-workers[30] proposed to assign the shoulders of the 691-cm^{-1} band to $\nu(C_a$–S), which is expected to occur in this region. At low temperature, the complex envelope resolves into three distinct bands (Figure 5). The 6-cm^{-1} ^{15}N shift identifies the 700-cm^{-1} band with ν_7, while 2–5 cm^{-1} downshifts upon C_a and C_b deuteration (Figure 15) identify the 692- and 682-cm^{-1} bands with C–S stretching. Astonishingly, the 692-cm^{-1} C_a–S stretch is the strongest band in the B-band-excited RR spectrum (Figure 3); enhancement is much weaker with Q-band excitation.

(29) Colthup, N. B.; Daly, L. H.; Wiberley, S. E. *Introduction to Infrared and Raman Spectroscopy*, 3rd ed.; Academic Press: New York, 1990.

(30) Srivastava, R. B.; Pace, C.; Yu, N.-T. *J. Raman Spectrosc.* **1981**, *11*, 20–23.

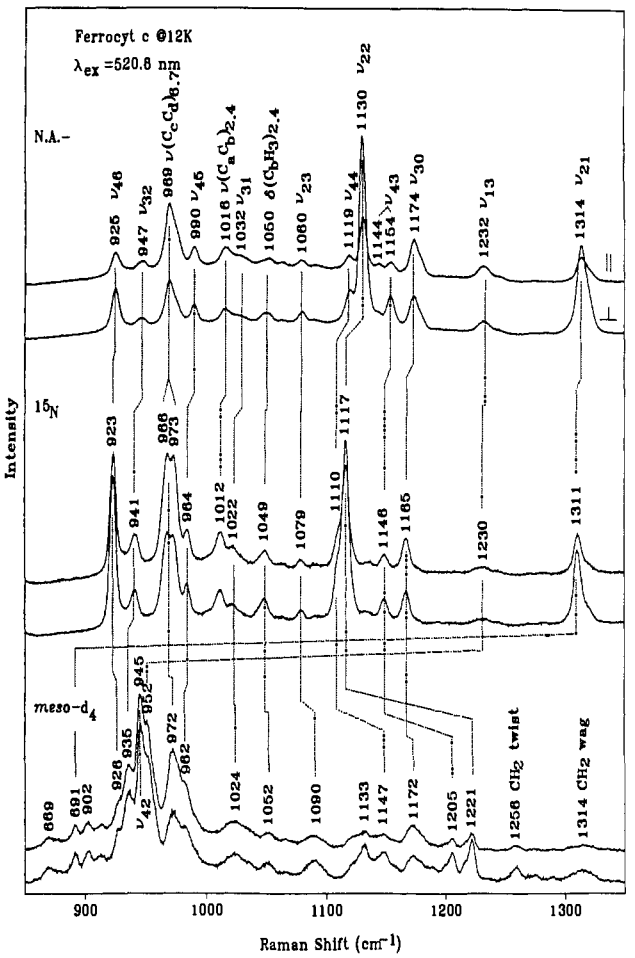

Figure 8. 520.9-nm excited resonance Raman spectra (850–1350 cm^{-1}) of natural abundance (N.A.), *meso*-d_4, and pyrrole-^{15}N ferrous cytochrome *c* at 12 K.

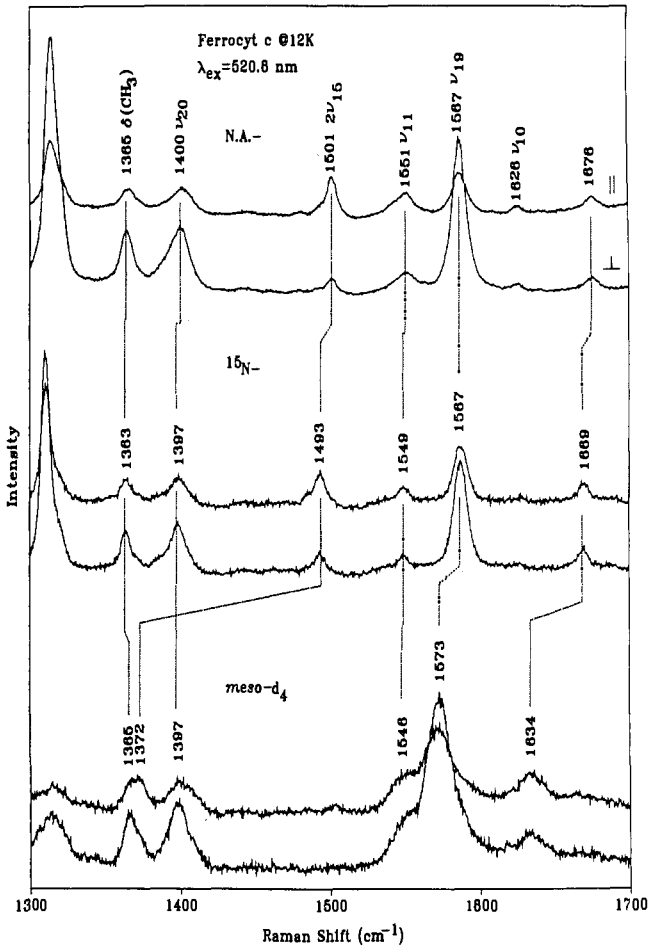

Figure 9. Same as Figure 8, but in the spectral region of 1300 to 1700 cm^{-1}.

$\delta(C_\beta–C_a–C_b)$ **and** $\delta(C_\beta–C_a–S)$. These heavy atom bending modes are assigned to the pair of doublets at 421/413 and 401/394 cm^{-1}. The former doublet shifts to 410/398 cm^{-1} upon C_b deuteration (Figure 15) and is assigned to $\delta(C_\beta–C_a–C_b)$. The 398-cm^{-1} band in the C_bD_2 spectrum is broad and probably covers the second doublet, shifted slightly in frequency; the second doublet is therefore assigned to $\delta(C_\beta–C_a–S)$.

B2. Propionate Modes. The propionate groups at the 6 and 7 positions resemble the ethyl groups in NiOEP, except for the substitution of a carboxylate group for a proton on the second carbon atom. In NiOEP, methylene modes have been identified at 1460 (scissoring), 1314 (wagging), and 1267 (twisting) cm^{-1} via methylene deuteration.[5b] These modes do not seem to be activated in cyt *c*, although the 1314-cm^{-1} position is obscured by the ν_{21} mode. In the *meso*-d_4 spectra, however, candidate bands for the methylene twist (1258 cm^{-1}) and wag (1314 cm^{-1}, the overlapping ν_{21} mode is shifted out of the region by *meso*-deuteration) are observed with Q-band excitation (Figures 8 and 11) and are anomalously polarized.

A pair of bands at 975 and 969 cm^{-1} is tentatively assigned to the propionate $C_c–C_d$ stretching vibrations, their frequency shifted down by the carboxylate substitution from the 1025-cm^{-1} value established for the NiOEP ethyl groups. The frequencies are nearly insensitive to the ring or 2,4-substituent isotope substitution, although they appear to collapse to a single band at 972 cm^{-1} in the *meso*-d_4 (Figure 6) or C_bD_2 (Figure 14) spectra. The bands are quite strong in both 413.1- and 520.8-nm excited spectra (Figure 3), reminiscent of the ethyl C–C stretches in NiOEP.[5b]

The pair of bands at 378 and 382 cm^{-1} are assigned to the $\delta(C_\beta–C_c–C_d)$ propionate bending modes, which have been located at 380 cm^{-1} in myoglobin via propionate deuteration.[31] These bands are nearly insensitive to the isotope labels on the ring or the 2,4-substituents (Figures 4 and 15).

B3. Ring-Adjacent Methyl Modes. In the methyl rocking region, weak features at 1063 and 1078 cm^{-1} are assigned to the methyl groups directly attached to the porphyrin ring, since they are affected only slightly by deuteration of the 2,4-substituents (Figure 14). There are no candidate bands for the out-of-phase C–H bends, but the in-phase bend (umbrella mode) is found as an anomalously polarized band at 1365 cm^{-1} with Q-band excitation (Figures 9 and 11). It shifts only 2 cm^{-1} upon ^{15}N substitution and is therefore clearly distinguishable from the coincident ν_4 mode, which gives rise to a very strong polarized band with B-band excitation; ν_4 shifts 7 cm^{-1} on ^{15}N substitution. The anomalous polarization of the methyl umbrella mode is attributable to vibrational mixing with A_{2g} skeletal modes, especially the strong ν_{21} mode at 1314 cm^{-1}.

C. Out-of-Plane Deformations. The low-frequency RR spectra contain additional bands which can be matched in frequency and isotope shift to out-of-plane (oop) deformation modes which have been assigned or calculated for NiOEP,[5c] as cataloged in Table III.

The highest frequency oop modes are the C_m–H wagging modes, $\gamma(C_m–H)$, at about 850 cm^{-1}. These modes are shifted out of the spectral region upon methine deuteration. The 413.1-nm excited spectrum (Figure 5) shows a weak polarized feature at 841 cm^{-1}. Upon the excitation at 530.9 nm (Figure 10), this band is replaced with an ap mode at 842 cm^{-1}, and a new polarized band appears at 826 cm^{-1}. These bands are absent in the *meso*-d_4 spectra; they

(31) Hu, S.; Spiro, T. G., manuscript in preparation.
(32) Schweitzer-Stenner, R.; Bobinger, U.; Dreybrodt, W. *J. Raman Spectrosc.* **1990**, *22*, 65–78.

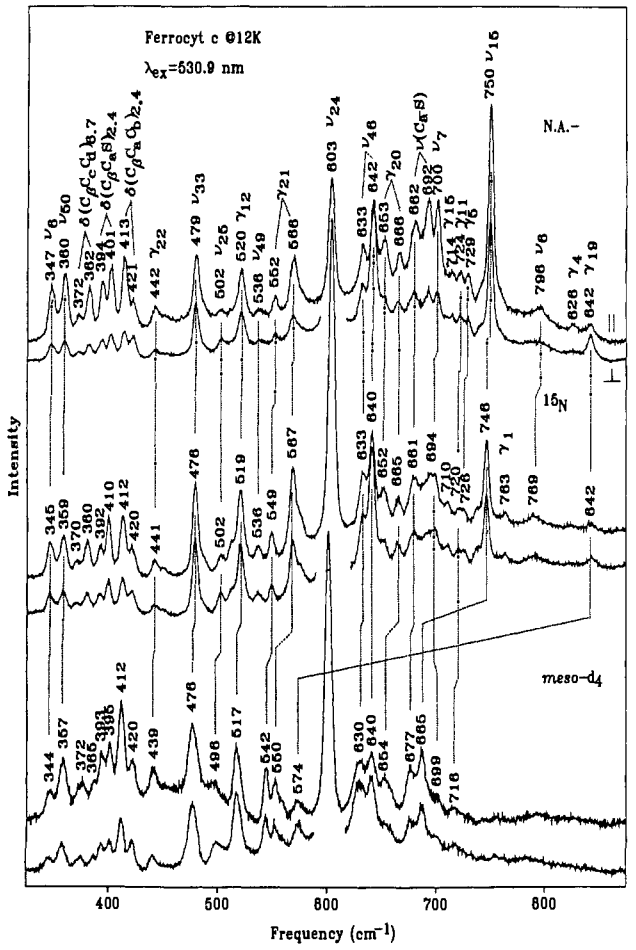

Figure 10. 530.8-nm excited resonance Raman spectra (325–875 cm^{-1}) of natural abundance (N.A.), *meso*-d_4, and pyrrole-^{15}N ferrous cytochrome *c* at 12 K. For clarity, the perpendicular trace of the ν_{24} band (603 cm^{-1}) was not shown.

Table III. Allocation of the Observed Out-of-Plane Modes of Ferrous Cytochrome *c* to the Local Coordinates[a]

local coordinates[b]	A_{1u}	A_{2u}	B_{1u}	B_{2u}	E_g
$\gamma(C_mH)$		γ_4 826 *844*	γ_{10} 841 *853*		γ_{19} 842 *841*
pyr fold$_{asym}$	γ_1 763 *750*		γ_{11} 724 *729*		γ_{20} 653/666 [*713*]
pyr fold$_{sym}$		γ_5 729 *739*		γ_{15} 714 *704*	γ_{21} 552/568 *656*
pyr swivel	γ_2 [*346*]		γ_{12} 520 *612*		γ_{22} 442 *492*
pyr tilt		γ_6 *360*		γ_{16} *270*	γ_{23} *254*
$\gamma(C_\alpha C_m)$		γ_7 [*284*]	γ_{13} [*130*]		γ_{24} *230*
$\gamma(C_\beta C_1)_{sym}$		γ_8 [*108*]		γ_{17} *127*	γ_{25} [*91*]
$\gamma(C_\beta C_1)_{asym}$	γ_3 [*74*]		γ_{14} [*44*]		γ_{26} [*63*]
pyr transl				γ_{18} [*30*]	
γ(NiN)		γ_9 [*32*]			

[a] The italicized values are those of NiOEP. The bracketed values are the calculated frequencies, for which the experimental values are not available. [b] For the definition of local coordinates of porphyrin out-of-plane vibrations, see ref 5c.

are thus assigned to the γ_4 (A_{2u}) (826 cm^{-1}), γ_{10} (B_{1u}) (841 cm^{-1}), and γ_{19} (E_g) (842 cm^{-1}) modes. A new ap band at 574 cm^{-1} in the 530.9 nm excitation spectrum of *meso*-d_4 cyt *c* may be the downshifted γ_{19} mode.

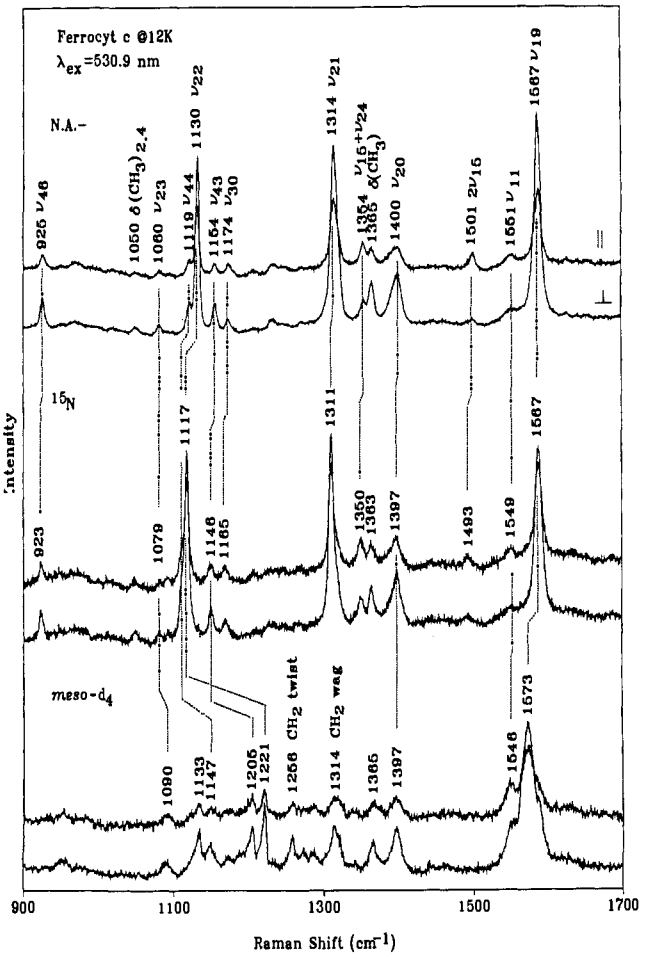

Figure 11. Same as Figure 10, but in the spectral region of 900–1700 cm^{-1}.

All of the expected pyrrole folding modes (both symmetrical and asymmetrical) are assigned to observed bands. The bands at 729 and 724 cm^{-1} in the 413.1- and 530.9-nm excited spectra (Figures 5 and 10) show 3–4-cm^{-1} ^{15}N downshifts and are assigned to γ_5 and γ_{11}, respectively. An additional band at 714 cm^{-1}, which can be assigned to γ_{15}, is only observed in the 530.9-nm excited spectrum. The highest frequency pyrrole folding mode, γ_1, is assigned to a band at 763 cm^{-1} in the ^{15}N isotopomer (Figure 10). As in the case of NiOEP,[5c] this band is not observed in the natural abundance spectrum because of overlap with the strong ν_{15} band at 750 cm^{-1}; ν_{15} weakens and shifts down slightly in the ^{15}N spectrum. The pairs of bands at 653/666 and 568/552 cm^{-1} are assigned to the two E_g pyrrole folding modes, γ_{20} and γ_{21}; lifting of their degeneracy is attributable to the heme distortion (see below). The two components of each pair show identical isotope shifts (Figures 5 and 10). Some of the pyrrole folding modes show substantial shifts upon 2,4-substituent deuteration (Figures 13 and 15). These shifts are expected because the pyrrole folding deformations are coupled to the bending of substituents.

Two of the three pyrrole swiveling modes are activated in the RR spectra. The γ_{22} (E_g) mode is assigned to the band at 442 cm^{-1}, while the γ_{12} (B_{1u}) mode is assigned to the band at 520 cm^{-1}. The latter band, which is strong in both the 413.1- (Figure 5) and the 530.9-nm excited spectra (Figure 10), shows 1-cm^{-1} ^{15}N and 3-cm^{-1} *meso*-d_4 downshifts. Although the ^{15}N shift is similar to that of NiOEP, the *meso*-d_4 shift is quite different. For NiOEP, γ_{12} is observed at 612 cm^{-1} for the natural abundance species and shifts *up* to 652 cm^{-1} in the *meso*-d_4 isotopomer, due to mode crossing with the $\gamma(C_m–H)$ mode, γ_{10}, which is downshifted from 853 to 501 cm^{-1}. There is no mode crossing in cyt *c*, since the natural abundance γ_{12} frequency (520 cm^{-1}) is below that of the downshifted γ_{10}; the latter is not observed,

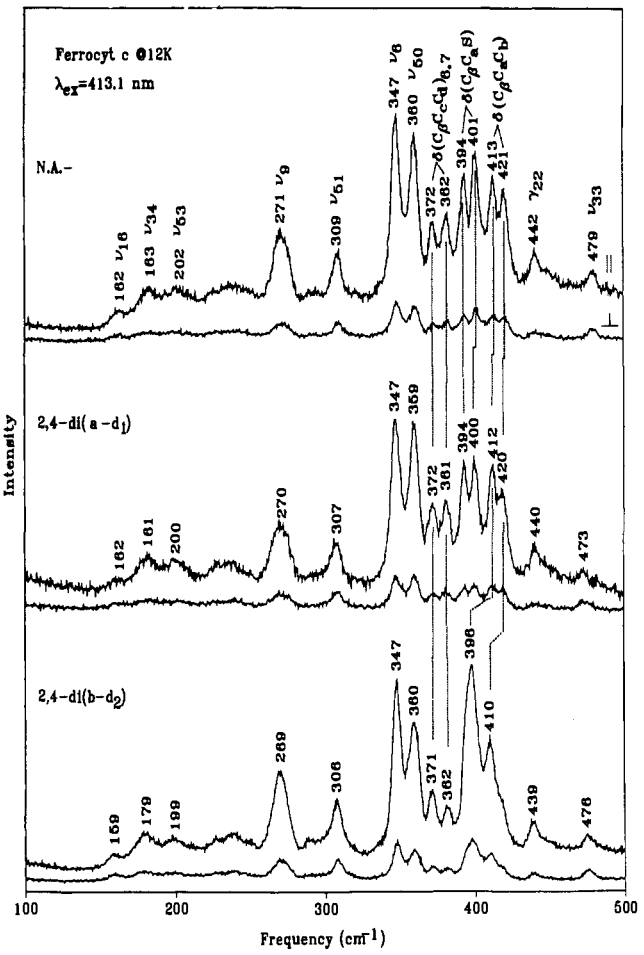

Figure 12. 413.1-nm excited resonance Raman spectra (100–500 cm^{-1}) of natural abundance (N.A.), 2,4-di(a-d_1), and 2,4-di(b-d_2) ferrous cytochrome *c* at 12 K.

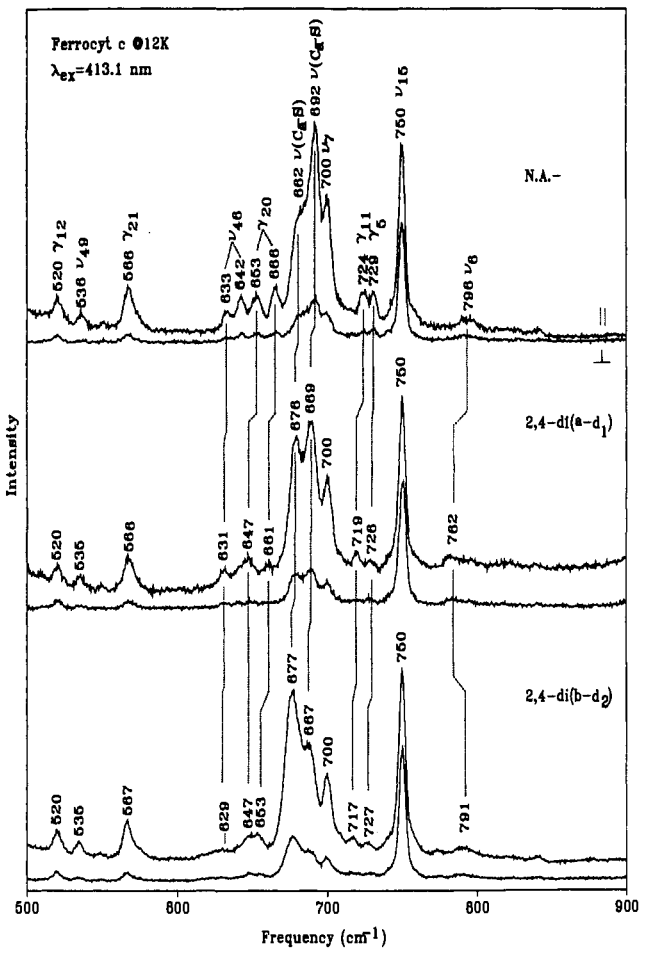

Figure 13. Same as Figure 12, but in the spectral region of 500–900 cm^{-1}.

but the frequency of another $\gamma(C_m-H)$ mode, γ_{19}, is located at 574 cm^{-1} in the *meso*-d_4 isotopomer.

D. Nonfundamental Vibrations. Nonfundamental vibrational modes of metalloporphyrins have previously been examined on several occasions. Friedman and Hochstrasser[27] suggested RR activity of overtone and combinations of the 752-cm^{-1} band. They pointed out that the nonfundamental vibrations are selectively enhanced with excitation near the Q_1 absorption region. Kitagawa and co-workers[33] extended the assignments of overtone and combination modes to several bands below 1700 cm^{-1} for NiOEP. Similarly, Bocian and co-workers[34] also proposed RR activity of some nonfundamental modes in the spectra of nickel 2,4-disubstituted deuteroporphyrin IX complexes. Many of these proposed nonfundamentals have, however, been allocated to ethyl internal modes in the recent NiOEP analysis of Li et al.[5b]

Nevertheless, several bands in the RR spectra of cyt *c* are attributable to nonfundamental modes from their isotope shifts. As suggested by Friedman and Hochstrasser,[27] the 1501-cm^{-1} band (Figure 11) is assigned to the first overtone of the ν_{15} (750 cm^{-1}) mode. This band is polarized (as expected of overtones, even of nontotally symmetric modes such as ν_{15}) and shows 8- and 129-cm^{-1} downshifts for ^{15}N and *meso*-d_4 isotopomers, respectively, nearly twice the isotope shifts of the ν_{15} fundamental (5 and 64 cm^{-1}). These shifts distinguish the ν_{15} overtone from fundamentals that are expected in this region, such as ν_{39} (not observed) or ν_3 (observed with 413.1 nm excitation). We note that a polarized band reported at 1502 cm^{-1} in the RR spectrum of NiOEP is also assignable to $2\nu_{15}$. It has the same (7 cm^{-1}) ^{15}N downshift. Moreover, it shifts up 4 cm^{-1} in methylene NiOEP-d_{16},[5b] which mirrors the observed upshift of ν_{15}, thus providing additional isotopic evidence for the assignment.

A weak band at 1354 cm^{-1} (Figure 11) can be assigned to the combination mode of ν_{15} and ν_{24} from its 4-cm^{-1} ^{15}N downshifts and disappearance upon *meso*-deuteration; the *meso*-d_4 shifted band is expected at 1289 cm^{-1} but is too weak to be observed. This band is depolarized, as expected for the combination (B_{2g}) of a B_{1g} and an A_{2g} mode. It is interesting to note that this band is only observed in the 530.9-nm excited spectrum. This is because the otherwise weak ν_{24} mode (624 cm^{-1}) becomes one of the strongest bands at this excitation.

Several bands (869, 902, 1133 cm^{-1}), observed in the 520.8- and 530.9-nm excited spectra of the *meso*-d_4 isotopomer (Figures 8 and 11), as well as the 1180-cm^{-1} band, observed in the 413.1-nm excitation RR spectrum (Figure 6) and showing a 5-cm^{-1} ^{15}N shift, are probably also nonfundamental modes.

E. Absence of Axial Ligand Modes. Cyt *c* has imidazole (His-18) and thioether (Met-80) axial ligands, and it would be of great interest to monitor the Fe–ligand stretching frequencies. We were unable, however, to find any candidate RR bands for these modes. They are expected to lie in the 200–400-cm^{-1} region. Fe–imidazole bands have been identified at 200–230 cm^{-1} for five-coordinate Fe(II) hemes[35a] and at 200 (symmetrical stretch)

(33) Kitagawa, T.; Abe, M.; Ogoshi, H. *J. Chem. Phys.* **1978**, *69*, 4516–4525.

(34) Willems, D. L.; Bocian, D. F. *J. Am. Chem. Soc.* **1984**, *106*, 880–890.

(35) (a) Kitagawa, T. In *Biological Applications of Raman Spectroscopy*; Spiro, T. G., Ed.; Wiley: New York, 1988; Vol. III, pp 97–131. (b) Mitchell, M. L.; Li, X.-Y.; Kincaid, J. R.; Spiro, T. G. *J. Phys. Chem.* **1987**, *91*, 4690. (c) Champion, P. M.; Stallard, B.; Wagner, G. C.; Gunsalus, I. C. *J. Am. Chem. Soc.* **1982**, *104*, 5469. (d) Bangcharoenpaurpong, O.; Champion, P. M.; Hall, K.; Hager, L. P. *Biochemistry* **1986**, *25*, 2374. (e) Schejter, A.; Lanir, A.; Vig, I.; Cohen, J. S. *J. Biol. Chem.* **1978**, *253*, 3768–3770.

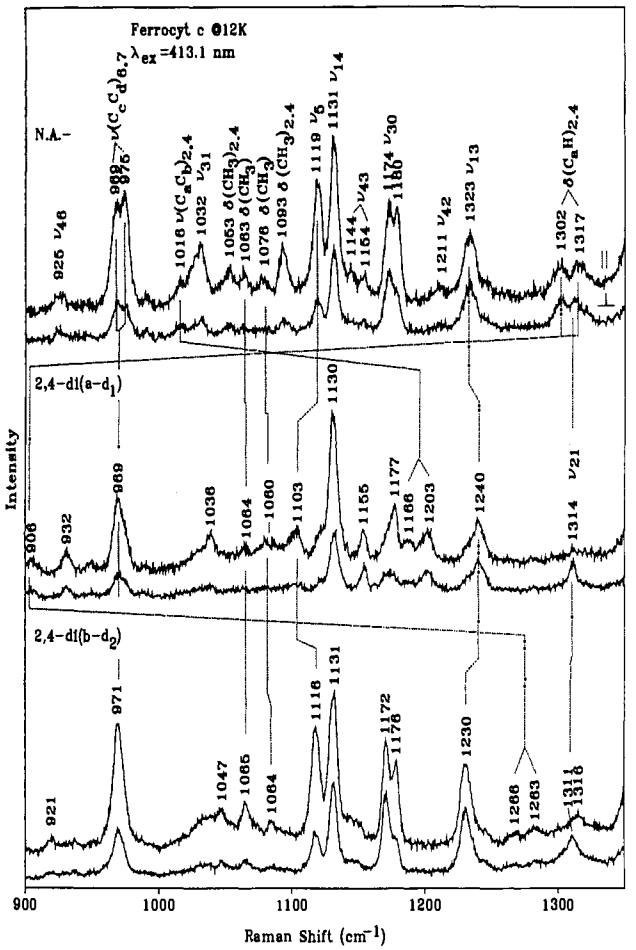

Figure 14. Same as Figure 12, but in the spectral region of 900–1350 cm^{-1}.

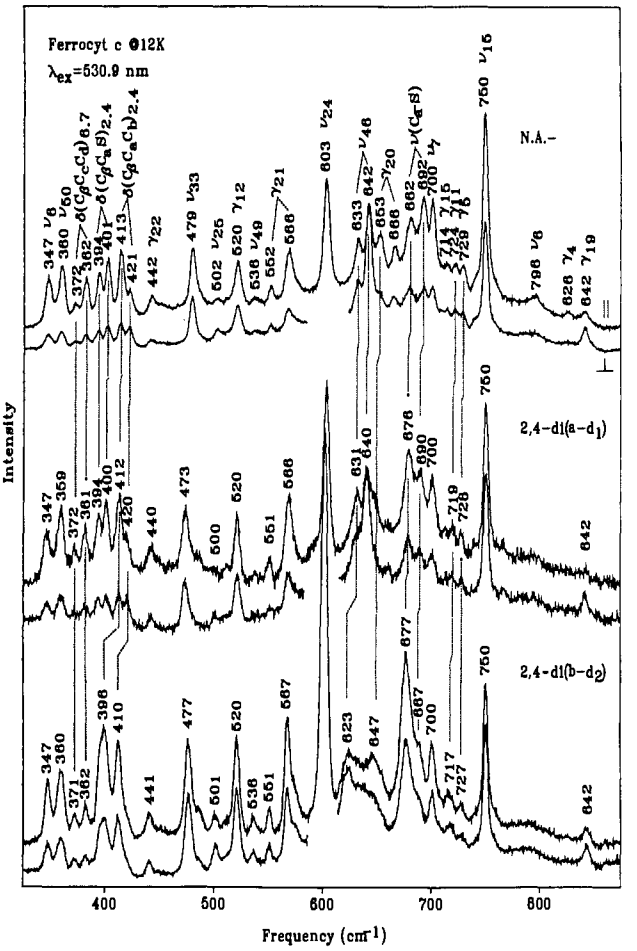

Figure 15. 530-nm excited low-frequency resonance Raman spectra (300–900 cm^{-1}) of natural abundance (N.A.), 2,4-di(a-d_1), and 2,4-di(b-d_2) ferrous cytochrome *c* at 12 K. For clarity, the perpendicular trace of the ν_{24} band (603 cm^{-1}) was not shown.

and 350 cm^{-1} (asymmetrical stretch) for $(ImH)_2Fe^{II}$protoporphyrin.[35b] Fe–thioether modes have not been identified, but the Fe–S(cysteine) stretch is at 350 cm^{-1} in five-coordinate Fe(III) cytochrome P450[35c] and chloroperoxidase.[35d] This region of the cyt *c* RR spectrum is crowded with bands, all of which have now been assigned to porphyrin or substituent modes. In an effort to uncover the Fe–S(methionine) stretch, we prepared cytochrome *c* in which the Met-80 methyl group is substituted by CD_3, via successive methylation–demethylation cycles with CD_3I.[35e] The labeled protein gave RR spectra (not shown) identical with those of unlabeled protein. We conclude that the Fe–axial ligand modes do not gain sufficient enhancement to be detected in the crowded spectrum.

F. RR Enhancement and Heme Distortion. In the main, cyt *c* shows the classical metalloporphyrin RR enhancement pattern[1] (Figure 3). Resonance with the strongly allowed B electronic transition enhances numerous polarized bands, representing normal modes along which the excited state is displaced (Franck–Condon scattering), while resonance with the quasiforbidden Q transition mainly enhances depolarized and anomalously polarized bands, representing nontotally symmetric modes which mix the Q and B states (Herzberg–Teller scattering). When the excitation is between the wavelength of Q_0 and its vibronic sideband Q_1 (530.9-nm spectra), then ap bands are selectively enhanced over dp bands by constructive and destructive interference, respectively, between the Q_0 and Q_1 contributions to the scattering.

There are, however, a number of anomalies in the cyt *c* enhancement pattern, which can be related to the heme distortion revealed in the cyt *c* crystal structure.[10f,g] As seen in Figure 1, the protein imposes a saddle geometry on the porphyrin ring, giving the chromophore a quasi-S_4 symmetry. The actual symmetry is, of course, lower than this, especially when the asymmetric dispositions of the propionate and $-CH(S)CH_3$ substituents are taken into account. In addition to the RR phenomena discussed below, the heme distortion may account for the red-shifted Soret band of ferrous cyt *c* (416 nm) relative to those of the ferrous forms of mesoheme-reconstituted cyt b_5 (410 nm)[36a] and microperoxidase-8 (411 nm),[36b] a heme-attached octapeptide derived from cyt *c*. Soret red shifts are observed for metalloporphyrins which are distorted as a result of substituent crowding,[37] e.g., octaethyltetraphenylporphine, and have been attributed to destablization of the π-electronic structure of the porphyrin, with a resultant increase in the energy of the HOMO relative to the LUMO.[38] The following RR anomalies are noted.

(1) The B-resonant spectra contain unusually strong dp bands. In fact, the B_{1g} pyrrole breathing mode ν_{15} (750 cm^{-1}) gives rise to one of the strongest bands (Figure 3). Activation of nontotally symmetric modes in B-resonant spectra has been attributed to the Jahn–Teller effect,[39] but the associated intensities (generally seen especially for ν_{10}, which is rather weak in cyt *c*) are usually modest. The very strong ν_{15} band suggests instead a vibronic mechanism, perhaps involving the two B transition components,

(36) (a) Ozols, J.; Strittmatter, P. *J. Biol. Chem.* **1964**, *239*, 1018–1023. (b) Harbury, H. A.; Loach, P. A. *J. Biol. Chem.* **1960**, *235*, 3640.

(37) (a) Shelnut, J. A.; Medforth, C. J.; Berber, M. D.; Barkigia, K. M.; Smith, K. M. *J. Am. Chem. Soc.* **1991**, *113*, 4077–4087. (b) Shelnut, J. A.; Majumder, S. A.; Sparks, L. D.; Hobbs, J. D.; Medforth, C. J.; Senge, M. O.; Smith, K. M.; Miura, M.; Luo, L.; Quirke, J. M. E. *J. Raman Spectrosc.* **1992**, *23*, 523–529.

(38) Barkigia, K. M.; Berber, M. D.; Fajer, J.; Medforth, C. J.; Renner, M. W.; Smith, K. M. *J. Am. Chem. Soc.* **1990**, *112*, 8851–8857.

(39) Shelnut, J. A.; Cheung, L. D.; Cheng, C. C.; Yu, N.-T.; Felton, R. H. *J. Chem. Phys.* **1977**, *66*, 3387.

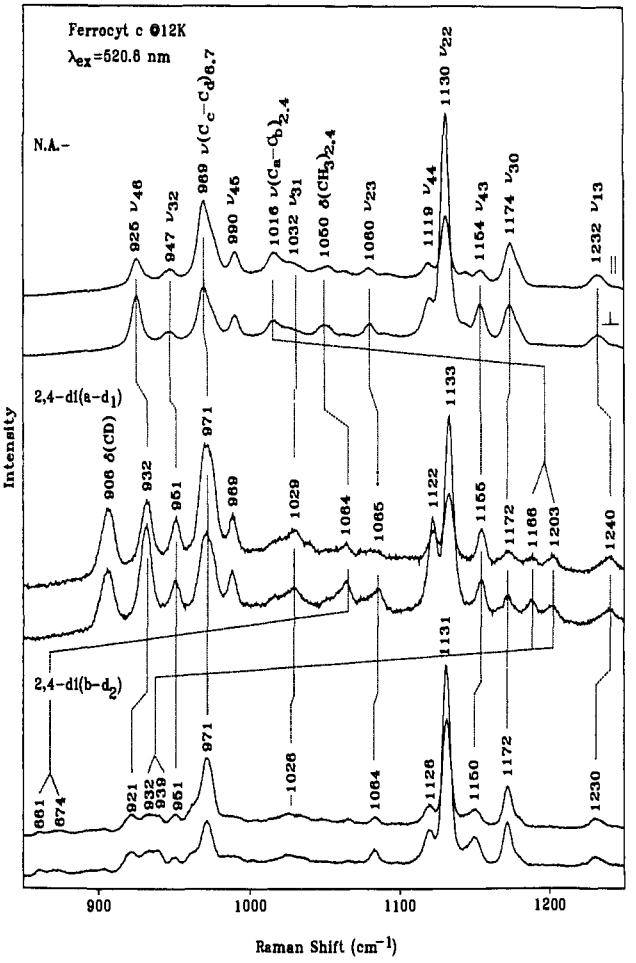

Figure 16. 520.8-nm excited resonance Raman spectra (850–1250 cm^{-1}) of natural abundance (N.A.), 2,4-di(a-d_1), and 2,4-di(b-d_2) ferrous cytochrome *c* at 12 K.

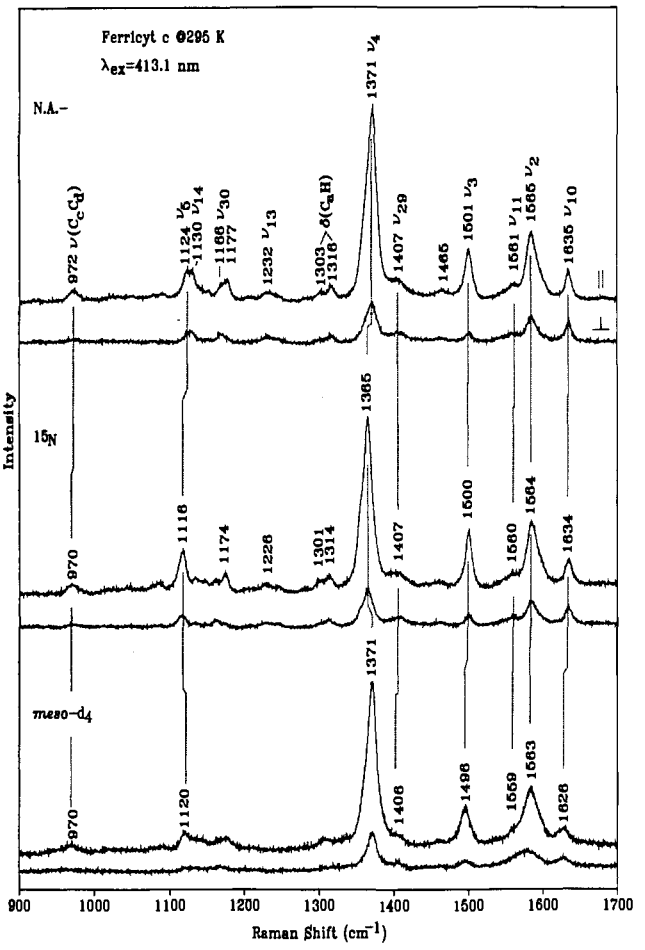

Figure 17. 413.1-nm excited resonance Raman spectra (900–1700 cm^{-1}) of natural abundance (N.A.), ^{15}N-, and *meso*-d_4 ferric cytochrome *c* at room temperature. The protein samples (about 50 μM), contained in a 5-mm NMR tube, were kept spining to avoid local thermal degradation and photoreduction.

B_x and B_y, which may be split by the symmetry-lowering. The B absorption band (Figure 2) is broad but has not been resolved, even at low temperatures. The Q_0 and Q_1 bands, however, do resolve at low temperatures into two components.[23]

(2) Anomalously polarized bands appear in the B-resonant spectra. Especially striking is the ν_{19} mode (1587 cm^{-1}), which produces one of the most prominent bands in the perpendicularly polarized spectrum (Figure 3). Another A_{2g} mode, ν_{21} (1314 cm^{-1}), is also detectable once the overlapping contribution from the $\delta(C_a–H)$ mode is removed by C_a deuteration (Figure 14). This phenomenon is most readily understood by recalling that in the S_4 (or any lower symmetry) point group, the A_{1g} and A_{2g} representations both correlate to A_1 and can therefore mix. This mixing permits Franck–Condon activation of the A_{2g}-derived modes via the saddling of the heme. (An alternative mechanism is again vibronic mixing of split B_x and B_y electronic transitions, but it is difficult to see why this mechanism should select for ν_{19} (A_{2g}-derived) over ν_{10} (B_{1g}-derived); both modes are asymmetric $C_a–C_m$ stretches with different phasing around the ring.) Consistent with this view are the observations that ν_{21} is also observed in the NiOEP B-resonant spectrum,[5b] and that it is stronger in tetragonal crystals, in which the porphyrin is known to be ruffled, than in solution.

(3) A number of out-of-plane modes are activated, in both B-resonant (Figure 5) and Q-resonant (Figure 10) spectra. These modes lack an enhancement mechanism in D_{4h} symmetry but can become Franck–Condon or vibronically active if the porphyrin undergoes an out-of-plane distortion. Many of them are activated in the ruffled form of NiOEP.[5c] We note particularly the prominence of the 568-cm^{-1} pyrrole folding mode γ_{21} in both B- and Q-resonant spectra (Figure 3). In ferric cyt *c*, this band is one of the strongest bands in the spectra (Figure 18) but is known to disappear upon unfolding of the protein[13] when the heme geometry is relaxed. Thus this band is directly tied to the protein-induced distortion.

(4) Many of the E_u-derived skeletal modes have been identified in the RR spectra, and two of them, ν_{43} and ν_{48}, are split into two components. The E_u band intensities are low, as expected for quasiforbidden modes, with the exception of ν_{50} and ν_{51} at 360 and 309 cm^{-1}, which are among the stronger bands in the B-resonant spectrum (Figures 3 and 4). They are nearly as strong as the adjacent A_{1g} modes, ν_8 and ν_9. Both pairs of modes are mixtures of Fe–N(pyrrole) stretching and porphyrin–substituent bond bending. For such modes, the distinction between the A_{1g}- and E_u-derived symmetries breaks down completely, because substituents across the porphyrin ring differ substantially.

In general, RR activation of E_u modes requires loss of the symmetry center of the chromophore and displacement of the excited state along the E_u-derived coordinate. E_u modes are seen in RR spectra of protoporphyrins,[7] and their activation is attributed to the conjugation of the asymmetrically disposed vinyl substituents with the porphyrin π system. When the vinyl groups are saturated in mesoporphyrin, the E_u modes disappear,[40] even though the substituents are asymmetrically disposed; π conjugation is required. Consequently, the electronic asymmetry imposed by the asymmetric disposition of the saturated porphyrin substituents in cyt *c* is insufficient to produce significant RR

(40) Spiro, T. G.; Burke, J. M. *J. Am. Chem. Soc.* **1976**, *98*, 5482–5489.

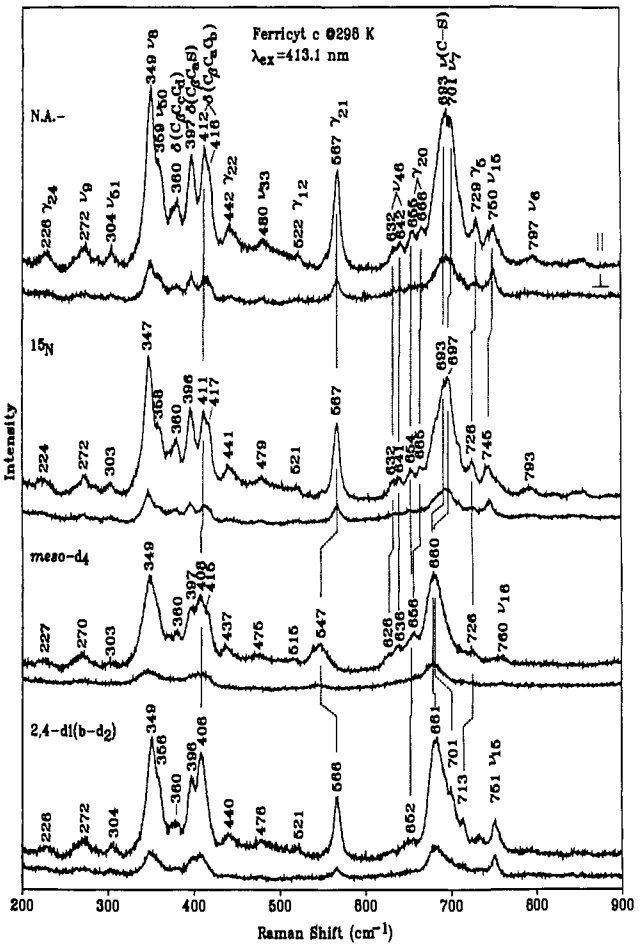

Figure 18. 413.1-nm excited resonance Raman spectra (200–900 cm^{-1}) of natural abundance (N.A.), ^{15}N, *meso*-d_4, and 2,4-di(b-d_2) ferric cytochrome *c*. Experimental conditions were the same as in Figure 17.

enhancement of the E_u modes (leaving aside ν_{50} and ν_{51}, for which the asymmetry is produced kinematically). Rather the activation must arise from the saddle distortion of the heme, which also destroys the symmetry center. Splitting of the E_u modes requires further that the *x*,*y* equivalence be destroyed, i.e., that the 4-fold rotation axis be lost. Thus, at least as far as the ν_{43} and ν_{48} modes are concerned, the effective heme symmetry is 2-fold or lower. Interestingly, both components of the ν_{43} mode, 1144 and 1154 cm^{-1}, are polarized with 413.1-nm excitation, but the 1154-cm^{-1} component becomes anomalously polarized with 520.8-nm excitation (Figure 8), presumably because of vibrational mixing with the strong A_{2g} mode, ν_{22}, at 1130 cm^{-1}.

This behavior of the 1154-cm^{-1} band is an example of polarization dispersion arising from symmetry lowering. But one must be careful about using depolarization dispersion as an indicator of symmetry lowering because of the possibility of mode overlap. For example, Schweitzer-Stenner and co-workers[32] have measured the wavelength dependence of the depolarization ratio of several cyt *c* RR bands and have fit the dispersion curves to fifth-order, time-dependent perturbation theory, with inclusion of multimode and vibronic coupling effects. Unfortunately, the four bands which they found to have large polarization dispersions, 1363, 1587, 1314, and 1177 cm^{-1}, are all subject to mode overlaps. The overlap of ν_4 and the methyl umbrella mode was pointed out above. The former, which is polarized, is resonant with the B excitation but is replaced by the latter, which is anomalously polarized in resonance with the Q transitions. This superposition is sufficient to explain the depolarization ratio varying from a value of ~1/8 in the B-excitation region to over 5 between Q_0 and Q_1.[32] Likewise, ν_{19} (ap, B- and Q-resonant) at 1587 cm^{-1} is overlapped with ν_2 (p, B-resonant) at 1592 cm^{-1}; ν_{21} (ap, Q-resonant) at 1314 cm^{-1} is overlapped with $\delta(C_a-H)$ (p, B-resonant) at 1317 cm^{-1}; and ν_{30} (dp, Q-resonant) at 1174 cm^{-1} overlaps with a band at 1180 cm^{-1} (p, B-resonant) which probably arises from a combination mode. On the other hand, the study by Schweitzer-Stenner and co-workers included three bands associated with relatively isolated modes, ν_{10} at 1626 cm^{-1}, ν_{11} at 1551 cm^{-1}, and ν_{13} at 1232 cm^{-1}, all of which showed little dispersion, with depolarization ratios clustered around 3/4, as expected for B_{1g} modes.

Another remarkable feature of the cyt *c* enhancement pattern is the prominence of substituent modes. The thioether C_a–S stretching band at 692 cm^{-1} is actually the strongest band in the B-resonant spectrum (Figure 3). The C_c–C_d stretches of the propionate groups, at 970 cm^{-1}, are also fairly strong. They are reminiscent of the ethyl C–C stretches in NiOEP, whose unexpected intensity was attributed to a hyperconjugation effect.[5b] Hyperconjugation might also account for the C_a–S stretch enhancement. Interestingly, the C_a–C_b stretches of the -C_aH(SR)$C_b$$H_3$ substituents, at 1016 cm^{-1}, are quite weak. It seems that the adjacent C_a–S bond stretches garner most of the intensity associated with these substituents. The C_β–C–C and C_β–C–S substituent bending modes between 370 and 420 cm^{-1} are also very prominent, however. It is evident that the cyt *c* π–π^* excited state undergoes a large displacement along these coordinates and also involves substantial C_a–S stretching.

G. Ferric Cyt *c*. RR spectra for ferric cyt *c* were only recorded at 413.1 nm, and only at room temperature (Figures 17 and 18), because it became apparent that the spectra are sufficiently similar to those of ferrous cyt *c* as not to pose any issues of mode assignment. The ^{15}N and *meso*-d_4 isotope shifts are essentially the same as those of corresponding bands in the ferrous cyt *c* spectra, and indeed, the frequencies are the same within 5 cm^{-1}, and usually within 1–2 cm^{-1}, for all bands below 1350 cm^{-1}. Even the relative intensities are nearly the same, the principal exception being that ν_{15} (750 cm^{-1}) is much weaker in ferric than in ferrous cyt *c*. In addition, the ν(C–S) band at 693 cm^{-1} is somewhat weaker and the γ_{21} band at 567 cm^{-1} is somewhat stronger in ferric than in ferrous cyt *c*. The multiplet structure of the 349–418 cm^{-1} band, though readily discernable, is less well resolved in ferric cyt *c*, partly because of slight band shifts, and partly because of band broadening at room temperature. The high degree of spectral similarity between the two oxidation states is in accord with the minimal change in heme geometry found in the high-resolution crystal structures.[10g]

Frequency shifts *are* seen for the high-frequency skeletal modes, as has long been known,[25] and are mainly due to a combination of core-expansion and more extensive Fe → porphyrin back-bonding in ferrous cyt *c*. ν_3 is sensitive only to core size, and the 5-cm^{-1} downshift from Fe(III) to Fe(II) is consistent with a slight (0.01 Å) expansion of the core.[3b] The 7 cm^{-1} reduction in ν_4 is mostly due to back-bonding, while the remaining high-frequency skeletal modes, ν_{10}, ν_{11}, and ν_2, are sensitive to both effects.[7]

Conclusions

The richness of the cyt *c* RR spectra arises from the prominence of substituent modes, especially those of the 2,4-thioether substituents, and from the activation of E_u-derived and out-of-plane skeletal modes, due to the protein-induced distortion of the heme. Enzymatic reconstitution with isotopically labeled hemes has permitted assignment of all the RR bands. These assignments will be important in applying RR spectroscopy as a structural probe of cyt *c* interaction with membranes[25k] and with the redox proteins.[11c-e]

Acknowledgment. This work was supported by Grant GM33576 from the National Institutes of Health (to T. G. S.).